The Dynamics of the User Effect on Electrically Small Antennas

Buskgaard, Emil Feldborg

DOI (link to publication from Publisher):
10.5278/vbn.phd.engsci.00166

Publication date:
2016

Document Version
Publisher's PDF, also known as Version of record

THE DYNAMICS OF THE USER EFFECT ON ELECTRICALLY SMALL ANTENNAS

BY
EMIL FELDBORG BUSKGAARD

DISSERTATION SUBMITTED 2016

AALBORG UNIVERSITY
DENMARK

The Dynamics of the User Effect on Electrically Small Antennas

Ph.D. Dissertation

Emil Feldborg Buskgaard

Dissertation submitted November, 2016

Dissertation submitted:	December 2016
PhD supervisor:	Professor Gert Frølund Pedersen Aalborg University, Denmark
Assistant PhD supervisor:	Associate Professor Gert Frølund Pedersen Aalborg University, Denmark
PhD committee:	Associate Professor Jan Hvolgaard Mikkelsen (chair) Aalborg University, Denmark
	Professor Lau Buon Kiong Lund University, Sweden
	Associate Professor Ville Viikari Aalto University School of Electrical Engineering, Finland
PhD Series:	Faculty of Engineering and Science, Aalborg University

ISSN (online): 2246-1248
ISBN (online): 978-87-7112-848-2

Published by:
Aalborg University Press
Skjernvej 4A, 2nd floor
DK – 9220 Aalborg Ø
Phone: +45 99407140
aauf@forlag.aau.dk
forlag.aau.dk

Printed in Denmark by Rosendahls, 2016

Abstract

The user effect on mobile phones has long been acknowledged as a major contributor to losses in cellular communications. Since the introduction of specific absorption rate (SAR) regulations, the model for quantifying these effects has been based on static measurements in controlled and reproducible environments. While this is a good approach for regulatory testing it is omitting much of the variance seen in a real-life scenario. In real life, the user will not use one static grip on the phone but will move the hand around on the phone in non-deterministic patterns. For classic antenna systems the antenna was a static structure without antenna tuning and therefore the user effect could not be compensated. The only focus was to guarantee that the SAR levels were lower than the legal limits and in some cases that the radiation pattern had a desired shape. For modern smartphones, the antenna system is getting increasingly tunable. This allows designers to consider feed-back systems that can compensate parts of the effect of the user. For such systems, a static user model is insufficient to test the efficiency of the regulation loop. Therefore, this study is focusing on the development of dynamic user effect models and measurement topologies. First a simulation model is presented where the index finger of a 3-dimensional hand model is parameterized. By moving the finger to several locations on the back plane of the phone, a first estimate of the user effect sensitivity of the phone can be obtained. The study presents simulated data for both single antenna systems and multiple input multiple output (MIMO) systems. For antenna measurements, the study introduces a novel device class, the tiny integrated network analyzer (TINA), that is a very small network analyzer used for measurements of the user effect inside of a mobile phone. This eliminates the need for external cables that are normally obstructing the user grip and adding cable effect. The device is finally used for a large-scale measurement campaign involving 100 test subjects performing various tasks on a mobile phone while the TINA is measuring the S-parameters of the phones' antennas. This study is the first to give actual measurements of the coupling between antennas on an electrically small antenna system as well as the first to give measured dynamic user effect data on a fully functional phone in a live network.

Resumé

En mobilbrugers inflydelse på mobiltelefonens antenner har længe været anerkendt som en betydelig kilde til degradering af signalerne i mobilnetværk. Siden introduktionen af specific absorption rate (SAR) regulativerne har tilgangen til kvantificering af brugerens interaktion med mobiltelefonen været baseret på statiske og reproducérbare modeller. Dette er en god tilgang til certificering hvor reproducibilitet er nødvendig, men det udelader megen af den varians som er til stede i et normalt brugsscenarie. En bruger vil ikke hold telefonen på een statisk måde men skift greb på telefonen på en vilkårlig måde. Tidligere var antennesystemerne i mobiltelefoner statiske metalstrukturer uden tuningskredsløb, som ikke kunne kompensere for brugerens effekt. Den eneste fokus for brugerinteraktionsmålinger var at garantere, at grænseværdierne for SAR var overholdt. Moderne mobilantenner bliver mere og mere tunbare. Derved åbnes muligheder for, at designere kan udvikle tilbagekoblingssystemer som kan kompensere for brugerens effekt på antennen. For sådanne systemer er en statisk model af brugerinteraktionen ikke tilstrækkelig til at test reguleringssløjfens effektivitet. Dette studie har derfor fokuseret på at udvikle dynamiske brugerinteraktionsmodeller of måletopologier. Første del af studiet præsenterer en simuleringsmodel af en hånd med en parametriseret pegefinger. Når fingeren flyttes til forskellige placeringer på telefonens bagside opnås et første estimat af telefonens følsomhed overfor brugerinteraktion. Dette studie præsenterer resultater for antennesystemer med både en og to antenner. Tuil måling af dynamisk brugerinteraktion præsenterer studiet en ny klasse af måleapparater, tiny integrated network analyzer (TINA), som er en yderst kompakt netværksanalysator, der kan foretage S-parameter-målinger direkte i en telefon uden brug af eksterne kabler. Dette apparat er blevet brugt i en omfangsrig målekampagne, hvor 100 brugere har udført forskellige opgaver på en mobiltelefon med TINA integreret. TINA har så løbende målt S-parametrerne for telefonen under forsøget. Dette forsøg er det første til at måle kobling mellem antenner for elektrisk små antennesystemer og samtidigt det første forsøg der har givet brugerinteraktionsdata for en fuldt funktionsdygtig telefon tilkoblet et offentligt mobilnetværk.

Contents

Thesis Details

Thesis Title:	The Dynamics of the User Effect on Electrically Small Antennas
Ph.D. Student:	Emil Feldborg Buskgaard
Supervisors:	Gert Frølund Pedersen, Aalborg University
	Ondrej Franek, Aalborg University

The main body of this thesis consists of the following papers.

[A] Emil Feldborg Buskgaard, Alexandru Tatomirescu, Samantha Caporal Del Barrio, Pevand Bahramzy, Ondrej Franek, Gert Frølund Pedersen, "Simple front-end concept for the complex challenges of multi-band communications," *The 9th European Conference on Antennas and Propagation (EuCAP) 2015*, pp. 1 - 5, 2015.

[B] Emil Feldborg Buskgaard, Alexandru Tatomirescu, Samantha Caporal Del Barrio, Ondrej Franek, Gert Frølund Pedersen, "User effect on the MIMO performance of a dual antenna LTE handset," *The 8th European Conference on Antennas and Propagation (EuCAP) 2014*, pp. 2006 - 2009, 2014.

[C] Emil Feldborg Buskgaard, Alexandru Tatomirescu, Samantha Caporal Del Barrio, Ondrej Franek, Gert Frølund Pedersen, "Effect of antenna bandwidth and placement on the robustness to user interaction," *International Workshop on Antenna Technology: "Small Antennas, Novel EM Structures and Materials, and Applications" (iWAT) 2014* , pp. 258 - 261, 2014.

[D] Emil Feldborg Buskgaard, Ben K. Krøyer, Alexandru Tatomirescu, Ondrej Franek, Gert Frølund Pedersen, "Tiny Integrated Network Analyzer for Noninvasive Measurements of Electrically Small Antennas," *IEEE Transactions on Microwave Theory and Techniques, 2016*, Volume: 64, Issue: 1, pp. 279 - 288, 2016.

[E] Emil Feldborg Buskgaard, Ben K. Krøyer, Ondrej Franek, Gert Frølund Pedersen, "Large-scale Experimental Study of the User Effect on Live

Mobile Phones," *IEEE Transactions on Antenna and Propagation, 2016*, Drafted.

This thesis has been submitted for assessment in partial fulfillment of the PhD degree. The thesis is based on the submitted or published scientific papers which are listed above. Parts of the papers are used directly or indirectly in the extended summary of the thesis. As part of the assessment, co-author statements have been made available to the assessment committee and are also available at the Faculty. The thesis is not in its present form acceptable for open publication but only in limited and closed circulation as copyright may not be ensured.

Preface

This thesis is submitted as partial fulfillment of the requirements for the degree of Doctor of Philosophy at Aalborg University, Denmark. The main part of the thesis is a collection of papers published in or submitted to peer-reviewed conferences or journals. It is the results of four years of research in the Section of Antennas, Propagation and Networking (APNet), at the Department of Electronic Systems, Aalborg University, in the period December 2012 - November 2016.

The contributions to this thesis were done under the supervision of Assist. Prof. Ondrej Franek and of Prof. Gert F. Pedersen, to whom I would like to express my sincere gratitude for sharing their expertise and enthusiasm. The work has been done within the Smart Antenna Front End (SAFE) project, funded by The Danish National Advanced Technology Foundation, during which a close collaboration with Intel Antenna Business and WiSpry Inc. has taken place. Through this collaboration, the deep insight of, amongst other, Poul Olesen, Boyan Yanakiev, Jørgen Bojer and Art Morris has been a great inspiration and lead to many of the presented results. I would also like to thank the my colleagues at APNet: Alexandru Tatomirescu, Samantha C. Del Barrio, Ehsan Foroozanfard and Wei Fan for their support and encouragement and for making the office an enjoyable place to come. Finally, a special thanks to Ben Krøyer and Peter Boie Jensen for their great effort in making the TINA measurement system possible and to my family and girlfriend, Bodil, and all of my friends for making the stay in Aalborg a great experience.

Emil Feldborg Buskgaard
Aalborg University, November 30, 2016

Part I

Introduction

Chapter 1

Introduction

1 Background of the Thesis

The smart phone has arguably become the most important technological advancement of the new millennium until now. The spread of mobile phones is epidemic and the extent of the societal dependency is monumental. This has resulted in very low tolerance to outages and therefore a very strong push for coverage all over the world. The guarantee for coverage comes at a price; The service providers need to invest heavily in infrastructure and the energy consumption of the worlds mobile networks increases rapidly. In the EU, the energy consumption of "Services", including communication systems was one of only two sectors to increase from 2012 to 2013 [1].

Much is being done to improve the efficiency of the base stations to deliver the required signal strength at minimal power consumption. But what if the signal strength requirement could be lowered by intelligent phone design? In a field where RF designers struggle to gain the last dB from the front-end, several dB can be easily lost in the antenna. The antenna efficiency drops particularly when the user interacts with the phone. Often more than 10 dB are lost due to the user where most is dissipated as heat in the body and some is due to dielectric loading of the antenna leading to mismatch loss.

Recent advances in RF front end technology has made antenna tuners a favorite with designers struggling to keep up with the ever increasing demand for bandwidth. These tuners are currently used for frequency reconfigurability only but could, with a mismatch feedback system, also be used to compensate the mismatch effect of the user. An important first step towards closed loop antenna tuning is to find the requirements for such a feedback loop. What range of mismatch can be expected and how fast will the feedback loop have to be to efficiently mitigate the effect of the user. This thesis aims to improve the methods of user effect simulation and measurement that

can be used to verify the reduction in power loss achieved by intelligent antenna design. The goal is to arrive at new and refined models and techniques for dynamic user effect investigation, both for simulation and measurement.

1.1 The extent of the user effect

It has long been a well known fact that the user has an adverse effect on the phone performance [2–6]. Studies have shown that the user can deteriorate the signal by more than 10 dB due to absorption and mismatch [7–9]. The issue is seen when the user handles the phone and the lossy tissue of the user's hands and head gets into the near field of the antenna. Much of the transmitted power will dissipate in the users head and hands as heat. Additionally, the dielectric constant of the tissue loads and mismatches the antenna.

1.2 Over-the-Air (OTA) testing

Because the user effect can be a significant part of the link budget in a cellular communication system, it is a part of the qualification test for a mobile phone [10–12]. The over-the-air (OTA) test measures the 3-dimensional radiation pattern of the antenna system under test. By subtracting the radiation pattern with the user from that of the antenna system in free space, the effect of the user is isolated. A model of the human head called a head phantom was developed in 1989 by the U.S. Army in the Anthropomorphic Survey (ANSUR) project [13] based on anatomic measurements of the heads of US Army personnel that were collected in 1988. This head phantom was dubbed the Specific Anthropomorphic Mannequin (SAM). As a large portion of the power loss for the user is lost in the hand, a hand phantom is also developed.

The Cellular Telephone Industries Association (CTIA) have defined a standardization test done in a controlled environment where the SAM phantom and the hand phantoms are used to mimic the effect of a real user [12]. To ensure that the head and hands are representative of the real world, the hands are molded from a compound that has electromagnetic properties similar to the real hands while the head is filled with a liquid that has the same properties and the real human head. A user grip study based on 100 test subjects [14], determined that, during a call, the grip style of all users can be divided into two styles: The soft grip and the hard grip. These are thus the two grips used for standardized testing.

The performance of the phone is measured over the air (OTA) in an anechoic chamber. This has enabled the quantification of the user effect and gives antenna designers a tool for optimizing antenna designs and positioning to minimize the degradation caused by the user. Other measurements have been done to determine the mismatching of the antenna using a wired setup to a VNA. This is difficult due to the effect of the coaxial cables needed

to connect the phone to the VNA [15]. The presence of metallic structures close to the antenna changes the antenna pattern and therefore also the user effect. It is thus not representative for the real performance to measure it this way. Therefore, almost all research of the user effect is simulation based or based on OTA measurements with the SAM and hands.

1.3 MIMO

In the constant hunt for more bandwidth, multiple input multiple output (MIMO) has enabled multiple streams of data to be transmitted to/from one mobile phone simultaneously on the same frequency [16]. This technology utilizes the difference between two radio channels that are uncorrelated to extract the two original data streams by digital post processing. The utilization of MIMO is only possible if the radio channels are not fully correlated and the less correlation between the channels the better [17, 18]. Another condition for MIMO is equal power in both MIMO channels. This difference in power is called the Branch Power Ratio (BPR) and it is calculated as the ratio between the path loss of one MIMO channel and the other. With the same noise floor for both channels, the BPR translate directly into the same difference in signal to noise ratio (SNR). For any channel the theoretical maximum throughput is dependent on the SNR. As a MIMO signal must be received through all channels to be decoded then the theoretical maximum throughput of the MIMO system is determined by the lowest SNR of all the channels. MIMO handsets are thus designed with two or more antennas that are as uncorrelated as possible and have similar radiated power efficiencies.

The user can deteriorate both correlation factor and BPR in a handset [19]. Studies show that highly decorrelated antennas become more correlated while highly correlated antennas become less correlated by the user. The user has thus an equalizing effect on correlation. With regards to BPR, the user will very often affect one branch more than the other leading to larger BPR and thus worse MIMO throughput.

1.4 Tunable antennas - a technology with possibilities

One interesting technological advancement is tunable antennas [20–23]. The ability to tune the antenna to the frequency of interrest means that the antenna designer can make smaller antennas that efficiently cover more bandwidth than non-tunable antennas can do. Smaller antennas have more stored energy compared to larger antennas [21, 24, 25]. This means that, if they are to be efficient, then the Q will be high for such antennas. This again means that their instantaneous bandwidth will be low so they are only able to cover a fraction of the desired bandwidth. By making the antenna tunable, the instantaneous bandwidth can be moved to the band of interest and the small

antenna can efficiently transmit and receive in the current band.

Two additional benefits arise from tunability when it comes to the user effect. Firstly, higher Q antennas have more confined near fields meaning that the phone is only sensitive in very small regions around the antennas [26]. The MIMO performance can also be improved since the antennas can be placed closer to each other without being strongly correlated [27]. Secondly, since the antenna is tunable it is possible to change the impedance of the antenna to account for the effect of the user. This would require additional circuitry to measure the effect of the user and determine the adjustment needed for the mitigation of the user effect [28].

When considering adaptive antenna tuning to mitigate the user effect, one problem arises: How can one measure the effect of the adaptive tuning and guarantee that it works as intended? As explained in Section 3, all current testing is based on static grips as these are easier to define. They will however not correctly guage the performance of an actively tuned antenna as the performance is not only a matter of statically optimizing the antenna but also requires a control structure to accurately measure and track the changes in the user effect. No currently used measurement method can test the antenna in this way. Furthermore, no measurements have documented the rate of change for the user effect so it is not possible to know if the effect can change instantly or the slope of the change is rather slow. This knowledge will be an important piece of the puzzle if adaptive tuning should be successful.

1.5 The SAFE concept and the user

This thesis is made as part of the Smart Adaptive Front-End (SAFE) project [20, 21, 29]. The core idea of SAFE is to shrink the antennas to the point where the bandwidth covers single channels rather than bands. For Frequency Division Duplexing (FDD) systems, the frequency offset between Rx and Tx means that one antenna can only cover either Rx or Tx. Therefore, a separate Rx and Tx antenna is needed but since they are both very small the combined volume of both antennas is still smaller than a conventional antenna. The two-antenna architecture utilizes the isolation achieved between the antennas as part of the duplex filtering. This relaxes the requirement to the duplex filter with 25 dB making it possible to use LC filtering instead of the typical surface acoustic wave (SAW) or bulk acoustic wave (BAW) filters used in normal designs. By utilizing the same type of tunable capacitors for the LC filter as for the tunable antennas, the whole Rx/Tx chain becomes fully tunable.

With a fully tunable Rx/Tx chain the need for many parallel Rx/Tx chains for separate bands and complex antenna switching is gone. The front end is then just split into one chain for high bands and one for low bands. The chains are fully independent and end in different small antennas. No switch-

ing required.

From a user effect perspective this topology is believed to have the benefits described in section 1.4 in vast amounts. The antennas are ultra high Q and therefore their stored energy is very closely distributed around the antennas. They are also highly tunable so the possibility is there to tune the antennas if the user affects them. However, the same challenges arise for the testing of such a system. There is a need to know how to measure adaptively tunable antennas and the basic behavior of the antennas in the hands of the user need to be understood better.

2 Aim of the Work

In this thesis, we focus on the interaction between the user of a mobile handset and the antennas inside the handset. Many studies have highlighted the health aspects of radiation of power into the human tissue [30–32]. This study will concern itself with the influence of the user on the phone instead. The user effect will be seen as a varying parameter that changes with the hand and head movements of the user. These fluctuations are of interest when designing modern MIMO antenna systems and when considering active antenna tuning. Therefore, simulation models and measurement techniques are investigated that can predict and measure the user effect dynamically as opposed to previous static user effect definitions and methods. The goals of this dissertation can thus be divided into the following partial goals:

Develop a simple and flexible simulation model. For any antenna design the first step is simulation. In this stage of a design, ideas will be explored in an iterative process. It is thus important to have simple simulation models that can quickly give a first estimate of the quality of a design. It must be repetitively applied to different designs to give the designer a basis for comparison. For this reason, we aim to provide a flexible but simple simulation model of the hand that can enable studies of the dynamic user effect early in the design flow.

Investigate the dynamic user effect versus antenna placement and Q. The placement of antennas on a mobile phone is already seen as an important factor for designers to obtain the best performance possible. It is well known that certain areas of a phone will be more sensitive to the user than other. Likewise, the bandwidth of the antenna determines how sensitive it will be to the user. For current antennas the bandwidth is given by the band requirements of the phone. With tunable antennas, the instantaneous bandwidth of the antenna can be reduced and for the SAFE architecture behind this project the bandwidth will be many times smaller. At the same time, more antennas will be required to

separate Rx and Tx leading to more locations on the phone being populated. One goal of this study is to investigate how these variations in bandwidth and placement affect the immunity to the user.

Investigate the dynamic effects of the user on MIMO systems. MIMO is becoming a prerequisite for many new communication standards and therefore it is crucial to examine the robustness of a MIMO antenna system to the dynamics of the user effect. For MIMO, multiple antennas have to work together in unity to communicate on several parallel channels. The user effect can affect both the correlation coefficient and branch power ratio (BPR) of the channels. If either of these parameters deteriorates significantly, the benefits of MIMO vanishes. Therefore, it is of interest to investigate how the BPR and correlation of the channels vary when the user grip changes.

Develop measurement system for dynamic user effect investigation. While simulation is a good tool for early stages of an antenna design, it is not able to fully predict the real world performance of a full system. Therefore, measurements are still the most important step in validating a design. Since the user effect is a very complex scenario to model the need for measurements is even greater. Currently no measurement system is able to assess the antenna performance in the presence of an actual user. This study aims to develop a system that can.

Measure dynamic user effect on electrically small antennas (ESA). When a system exists that can actually measure the performance of an antenna system in the presence of a real user then it opens the doors to many previously impossible investigations. First and foremost, the ability to measure not only the static detuning of the antenna by the user but also to track the rate at which the detuning changes gives very important input for any designer considering to employ active antenna tuning to combat user effect.

Measure the dynamic user effect on MIMO performance. It is to this point not possible to measure S21 correctly on ESA since the measurement system will influence the measurement results and thereby invalidate them. When a new measurement device is designed that can truly measure phone performance without cables or any other major changes to the design then it will be possible for the first time to obtain measured data for the S21 between MIMO antennas on a real mobile handset while handled by the user.

3 State of the Art

The user effect is currently mostly studied as a static quantity. Both in simulations and measurements the user is substituted by a static model. In the following sections, the currently used techniques for user effect studies are explained.

3.1 Specific Absorption Rate (SAR)

For many years, the most important figure of merit for user effect has been the specific absorption rate (SAR). It is specified in the specifications of both the Federal Communications Commission (FCC) [10] and the European Telecommunications Standards Institute (ETSI) [11]. The limits to SAR are set based the radiation levels that are considered safe and is measured in either 1.6 W/kg in 1 gram or 4 W/kg in 10 grams [33]. The toughest requirement is the limit of 1.6 mW/g in 1 gram.

The actual measurement is conducted in a big vat of liquid [34]. The phone is attached on the outside underneath the vat The liquid is a saline solution that has electromagnetic properties closely matching those of the human body. A field probe is navigated around in the saline solution scanning the volume close to the phone and measuring the field strength at different points inside the liquid. The vat bottom can be either flat or shaped like a human torso.

These measurements are more concerned with the health issues of using the phone than the user effect on the antennas in the phone. The scope of this study is more on the user effect on electrically small antennas and therefore the next section will describe a setup commonly used for these types of measurements.

3.2 Ovet the Air (OTA) Measurements With Specific Anthropomorphic Mannequin (SAM)

One measurement approach prevails for the user effect on handset performance: Over-the-air (OTA) measurements [7–9]. The OTA measurements are conducted in shielded and anechoic rooms, lined with absorbing foam cones. The DUT is placed in the middle of the room and measured from a grid of positions forming a sphere around the DUT. The output of this measurement is a complete pattern of the radiation from the phone in 3 dimensions (3D). This antenna pattern tells both about the directivity and the losses of the antenna system.

For user effect measurements, a structure is used to mimic the effect of a user. This can be either flat block, a full body phantom or a partial body

phantom. A commonly used model is the Specific Anthropomorphic Mannequin (SAM) [13] this is a head with neck mounted on a pedestal. Along with the SAM hand models are used that are wrapped around the phone. Both tight and loose grip hands are used as these two grip styles have been determined to cover the vast majority of all users grips. Both left and right hands are used as well. Common for all of these structures is that their electromagnetic parameters are designed to match those of the human body.

With these measurements, a very detailed analysis of the antenna system can be made. It can be seen both how the presence of the user changes the radiation pattern of the phone in 3D and how much power is lost due to the presence of the user. The drawback is that the measurement takes a considerable amount of time to complete due to the scanning of the probe antenna around the phone. For the duration of the sweep, the setup must be completely static in order for the pattern to be useful. Also, for very directive antennas or antennas with sharp nulls, a very fine spatial resolution is required to ensure that all extrema are found and to ensure the correct integration of power.

Another approach is based on S-parameter measurements and that will be explained in the following section.

3.3 Vector Network Analysis (VNA)

For quick measurements, many antenna designers rely on S-parameters for early evaluation of a design. The S-parameters are measured with a measurement device called a vector network analyzer (VNA). The VNA is able to generate an RF signal, feed it to a port of the DUT and measure the reflected power with both amplitude and phase information. Additionally, it can often measure the power coupled to one or more other ports of the DUT. In this way, an S-parameter matrix is obtained that can tell the designer about the quality of the matching of the antenna and the isolation between ports.

These measurements require much less of the measurement environment than OTA measurements. They can be done on a lab bench and provide quick feedback to the antenna designer. A sweep generally takes much less than a second where an OTA sweep can take several minutes.

These measurements only provide information about the reflection and coupling coefficients of the antenna system. They do not measure the complete loss. It is however the reflection coefficient that can be directly modified using antenna tuning. It is thus the right parameter to measure for anyone interested in seeing if their tunable antenna covers the frequency range of interest.

The largest drawback of VNA measurements - especially on electrically small antennas - is that there needs to be a cabled connection between the DUT and the VNA. The normal and simple solution is to use a coaxial cable

directly from the VNA to a connector on the DUT antenna system. This solution brings a metallic structure, the cable, into the near field of the antenna. Some of the fields radiated from the antenna and some of the currents running on the metallic structure of the DUT will creep onto the coaxial cable. This results in changed impedances and the coaxial cable is now effectively a part of the radiating structure.

Some studies [35–37] have tried to prevent this by using an RF to optical converter and establish the link between the VNA and the DUT as an optical link through non-metallic fiber-optic cables. Here, the cables exert minimal influence on the radiation of the DUT which is good. The RF to optical converter is however a very big structure with metallic parts that in itself will have an influence on the measurements.

For user effect measurements, the VNA based measurements have long been less popular since the cables are often in the way of the desired grip on the phone. It is however a quick way to get a first impression of the sensitivity of an antenna to the user, simply by touching the antenna system and looking at the changes in S-parameters on the screen of the VNA.

4 Contribution

The papers included in this thesis are briefly summarized in this chapter. The motivation for each individual contribution is described along with their main results and how they are linked to the other contributions.

Paper A

Simple front-end concept for the complex challenges of multi-band communications
Emil Feldborg Buskgaard, Alexandru Tatomirescu, Samantha Caporal Del Barrio, Pevand Bahramzy, Ondrej Franek, Gert Frølund Pedersen
The paper has been published in the proceedings of *The 9th European Conference on Antennas and Propagation (EuCAP) 2015*, pp. 1 - 5, 2015.

Motivation

This PhD dissertation is produced as part of the SAFE project. It is therefore important to have a good understanding of the aim of this project to be able to put the study into context. The project has been running since 2010 and a substantial amount research has been done into miniaturized high-Q antennas. Therefore an intensive study of the motivation behind the project and the proposed architecture is done. The main objective of SAFE is to simplify the front-end architecture and reuse the transceiver chains for more bands by making them tunable.

Paper content

This paper proposes a new architecture for mobile phone front-ends that dramatically reduces the complexity of multi-band smart phones. Traditional smart phone front-ends consist of many parallel transmit (Tx) and receive (Rx) chains dedicated to the different bands. The proposed architecture simplifies this by making the few fully frequency tunable Tx and Rx chains that each cover multiple bands.

Three implementations of antenna systems for the proposed architecture are shown and discussed. They all consist of separate Rx and Tx antennas with more than 25 dB of isolation in between. Combined with additional tunable Rx and Tx filters the Rx/Tx isolation reaches 50 dB which is comparable with the isolation achieved with commercially available static duplex filters.

Based on these antenna designs it is concluded that the proposed architecture is feasible for LTE phones and makes full band coverage realistic. Current 5G investigations show that the advantages of flexible front-ends will be even bigger as technology moves toward software defined radio.

Main results

This paper manages to show an alternative to the state-of-the-art front-end where fixed duplexers using SAW or BAW filters dictate the use of separate transceiver chains for each band. In technologies such as LTE where a wide selection of bands are available the possibility to reuse the same transceiver chain for more bands is very attractive.

Paper B

User effect on the MIMO performance of a dual antenna LTE handset
Emil Feldborg Buskgaard, Alexandru Tatomirescu, Samantha Caporal Del Barrio, Ondrej Franek, Gert Frølund Pedersen
The paper has been published in the proceedings of *The 8th European Conference on Antennas and Propagation (EuCAP) 2014*, pp. 2006 - 2009, 2014.

Motivation

In realization of the fact that the tunability of antennas can be used for actively mitigating the user effect, the question is how much can be gained from such active antenna tuning. This depends on the extent of the user effect which is phone design dependent. Therefore the decision to employ active antenna tuning must rely on an estimate of the user effect. The current way of estimating user effect is based on the CTIA hand and head phantoms that are static in nature. They are thus not giving any information about the fluctuations of the user effect for changes in the grip by the user.

This study ventures into the area of dynamic user effect estimation by deriving a simple first quasi variant model of the user effect. The aim is to make a simulation model for the user hand that is dynamic yet reproducible and anatomically correct. With this hand the effect of the user effect is studied on a MIMO handset antenna system.

Paper Content

The paper introduces a simulation model of a head and hand derived from the CTIA specification [12]. The head is a precise replica of the CTIA head phantom while the hand has a modified index finger. The index finger has the same material parameters as the standard CTIA hand but it is built from spheres and cone stubs that are all parameterized such that they can be moved by adjusting their parameters. The parameters are made such that, within a certain range, a coordinate on the back plane of the phone can be entered and the finger will move to this position.

For this paper, a MIMO antenna system for LTE band 13 is developed. The antennas are centered at 751 MHz and have adequate MIMO performance in free space. They are wrapped inside a box modeling the plastic enclosure of a smart phone. The phone model is simulated both in free space and next to the head and hand phantoms. The index finger of the hand phantom is moved to six different positions.

Main Results

The outcome of the simulation study was that the finger position did indeed play a role in the MIMO performance of a two-antenna system in a handset. The main part of the user effect is due to absorption which is present no matter where the index finger moves but there is a clear difference in branch power ratio and antenna isolation due to the finger placement.

Paper C

Effect of antenna bandwidth and placement on the robustness to user interaction

Emil Feldborg Buskgaard, Alexandru Tatomirescu, Samantha Caporal Del Barrio, Ondrej Franek, Gert Frølund Pedersen

The paper has been published in the proceedings of the *International Workshop on Antenna Technology: "Small Antennas, Novel EM Structures and Materials, and Applications" (iWAT) 2014* , pp. 258 - 261, 2014.

Motivation

Using the simulation model of the hand with the reconfigurable index finger from Paper B, a new simulation study is performed. This study is concerned with the Q and the placement of the antenna. It has long been seen as good design practice to place the antenna of a handset at the bottom of the handset to maximize the distance from the radiating structure to the head. This study aims to answer whether this approach is also beneficial for minimizing the variance of the user effect when the index finger is moving. Additionally, the study aims to investigate the effect of the antenna Q on the variance of the user effect due to the moving index finger. This is of interest since the higher Q antenna will have more closely confined fields. It is thus expected that the finger will have to go closer to influence the antenna making it less sensitive. At the same time the high Q antenna has stronger fields close to the radiating structure and is thus expected to be more sensitive to the user touching right on the radiating structure than a low Q antenna would be. It is important to the SAFE project to test this hypothesis.

Paper Content

The paper outlines the simulation model of the hand and introduces two antenna systems, a high Q antenna and a low Q antenna. Each antenna is attached to a ground plane and placed inside a plastic housing with 1 mm from the metallic parts to the outside of the housing. The antenna systems are placed inside the simulated hand with the antenna either at the top (close to the finger tips) or at the bottom (close to the palm of the hand).

Based on these 4 combinations of antenna Q and placement, simulations are done and the effect of the moving finger is recorded for 6 finger positions.

Main Results

The study found that the detuning of the antenna was strongly dependent on Q and less so on the placement of the antenna. Mismatch was affected by both placement and bandwidth. The sensitivity to the finger movement was much larger with a top mounted antenna which makes sense sing the index finger directly touches the antenna region. For the absorption, the placement was found to be more important than the Q of the antenna.

Overall losses were a lot higher for top mounted antennas than for bottom mounted antennas. This supports that placing the antenna at the bottom of the phone is the right design choice for smartphones.

Paper D

Tiny Integrated Network Analyzer for Noninvasive Measurements of Electrically Small Antennas
Emil Feldborg Buskgaard, Ben K. Krøyer, Alexandru Tatomirescu, Ondrej Franek, Gert Frølund Pedersen
The paper has been published in *IEEE Transactions on Microwave Theory and Techniques, 2016*, Volume: 64, Issue: 1, pp. 279 - 288, 2016.

Motivation

Based on the simulation studies it is clear that there is some effect of the user that is dynamically changing when the user changes grip. It has however been impossible to validate these findings with the measurement tools available to the engineering world so far. The two dominating antenna measurement methods are OTA and VNA measurements as described in Sections 1.2 and 1.3. The OTA method is too slow to capture dynamic behaviors and the VNA relies on cables leading to cable effect. If fiber optics are used for the VNA, the cable effect can be removed but all current fiber optics converters still need a sizable box with metallic shielding that will influence antenna performance. On top of this the cables or fibers leaving the phone will substantially change the appearance and user experience of the phone leading to non-natural user grips.

There is thus a need for a new measurement method if the user effect should be measured dynamically. This study proposes such a system, the Tiny Integrated Network Analyzer (TINA). The aim of the study is to investigate the performance of this new system to evaluate its feasibility. The TINA is an ultra-compact network analyzer that fits inside the DUT making it possible to fully eliminate cables and make the DUT look and feel completely as if the TINA was not there. This enables the most realistic user experience possible and thus the most correct user interaction.

Paper Content

The paper contains a detailed description of the TINA and the design considerations that went into its creation. The system consists of off-the-shelf components with known non-idealities. Therefore the design has to take these issues into account and find work-arounds for them. Some are handled by hardware work-around, others are handled by calibration and post processing. Generally the design philosophy is that as much as possible of the intelligence of the system must be placed in the calibration of the system and the post processing of the measurement data in order to simplify the TINA itself as much as possible. This helps keeping the design compact and power

efficient. The paper further explains a test bed that has been developed based on an iPhone 5 to house the TINA and test it in the intended scenario.

The TINA is tested to guage the performance and feasibility of the system. First the calibration is tested for repeatability and its ability to predict a certain impedance on the lab table. Thereafter the TINA is implanted in the iPhone 5 and subjected to a series of grips. The result of this is a series of S-parameters that have been analyzed to conclude on the quality of the system.

Main Results

The study has shown that it is possible to create an ultra-compact network analyzer and completely hide it inside a fully functional phone. The performance of the system is not to be compared to a commercially available network analyzer but it is good enough to give an indication of the dynamics of the user effect that is otherwise impossible to get.

Paper E

Large-scale Experimental Study of the User Effect on Live Mobile Phones
Emil Feldborg Buskgaard, Ben K. Krøyer, Ondrej Franek, Gert Frølund Pedersen
The paper has been submitted December 4th 2016 to *IEEE Transactions on Antenna and Propagation, 2016*.

Motivation

Based on the successful implementation of the TINA, a host of new possibilities for measuring user effect unfold. Effects that were previously speculative can now be measured in practice. Of these effects especially two are of interest: the coupling between antennas in a MIMO handset and the range and rate of change for the reflection coefficient on the transmit antenna of a handset. The coupling is of interest since it is impossible to measure in a setup with cables as these cables have a large effect on the coupling for electrically small antenna systems.

The reflection coefficient is important since it is the figure that potentially can be compensated by closed loop antenna tuning. In order to determine the range and rate of change of the reflection coefficient, one need to subject the antenna system to the varying data grips of a user and collect a time series of data. This data must be used in a statistical way to extract the desired quantities.

Paper Content

This paper describes the setup, execution and results of a large-scale user study carried out on a modified iPhone 5s with the TINA integrated. The study was performed in a test room where the test subjects were asked to make a call on the phone and perform various tasks while in call mode. The tasks were to talk, write an SMS with the phone in portrait mode, write an SMS with the phone in landscape mode, scroll on a homepage and plug in the charger. By performing all of these tasks, the user was forced to move the hands to different grips. The study was performed on 100 test subjects to give a large statistical basis for the further data analysis.

Main Results

The user study yielded many novel results. For the coupling between antennas on an electrically small handset these were the first results of their kind. The results showed a very low coupling for the iPhone 5s of less than -30 dB for more than 75 % of the data. For reflection, the study showed poor performance for the low European 2G band with more than 75 % of the reflection coefficients being larger than -6 dB. For the high European 2G band, the reflection coefficients were much better and the spread was much smaller.

Additionally a dependency on power level was found that is believed to be a second order effect from the frequency dependency and thus not directly related to power level. A dependency on gender was identified and could be explained by the difference in hand size between men and women.

For the rate of change, certain events were identified that led to extremely fast changes in S-parameters. These changes were linked to the movement of the test subjects hand onto or away from the points on the bezel where the antenna meets the ground plane. This is believed to be the points with the highest electromagnetic fields and therefore the points that were expected to be highly sensitive. The fastest changes recorded were around 0.2 s from -2 dB to -6 dB.

5 Conclusion

This study set out to expand the knowledge about the dynamics of the interaction between the user and the mobile phone. The previous modeling was built on static scenarios that worked well for static antenna systems but have shortcomings when antenna systems become adaptive. The study introduces two new methods to analyze user effect; a simple and repeatable simulation model that can be used for comparative studies of antenna designs and placement early in the antenna design cycle, and a measurement system the

can be used to measure performance of the finished antenna design that was previously impossible to measure.

These systems have both been used to gain new insights into the dynamic user effect. The simulation model was used to determine that high Q antennas are less susceptible to user interference and that placing the antenna at the bottom of the phone is preferable to placing it at the top. The same model was used to study a MIMO antenna system which led to the conclusion that the user increases the Branch Power Ratio significantly while helping to decorrelate the antennas.

The measurement system, the TINA, was devised, built and verified in the course of this study. The system is the first of its kind and does exhibit some non-ideal behavior. It is also not trivial to integrate in a commercial phone and it is therefore mostly justified by the fact that nothing else is able to measure the dynamic user effect on electrically small antennas at the moment. There is reason to believe that this class of measurement devices will be increasingly accurate as closed loop antenna tuning systems are likely to need network analysis to measure the mismatch as the feedback of the loop.

The TINA is further used to study the user effect on an iPhone 5s in a large study with 100 users. The study was blind which was only possible due to the full integration of the measurement system inside the phone. The study concluded that the transient speed of changes in S_{11} is worst case in the order of 200 milliseconds for a step from -6 dB to -2 dB. S_{11} was generally found to be worse in low band compared to high band and influenced by parameters such as gender of the user and transmit power level. The S_{21} of the phone is generally lower than -30 dB which is a surprisingly low coupling.

As a whole, this Ph.D. study managed to deliver new solutions to the realm of user studies. The need for dynamic simulation models and measurement tools was identified in the advent of closed loop antenna tuning. First steps were taken towards a more realistic approach to user effect evaluation, both in simulations and measurements. The technologies developed during this Ph.D. study are early versions with great promise but also definite issues. The Ph.D. student is excited to follow the development in this field and discover where the research in dynamic user effect will evolve over the coming years.

References

[1] E. E. Agency. (2016, October) Final energy consumption by sector and fuel @ONLINE. [Online]. Available: http://www.eea.europa.eu/data-and-maps/indicators/final-energy-consumption-by-sector-9/assessment

[2] G. Pedersen, "Antennas for small mobile terminals," Ph.D. dissertation, Aalborg University, 2003.

[3] M. Pelosi, "User's influence mitigation for small terminal antenna systems: Ph.d. thesis," Ph.D. dissertation, Aalborg University, 2009.

[4] P. Eratuuli, P. Haapala, P. Aikio, and P. Vainikainen, "Measurements of internal handset antennas and diversity configurations with a phantom head," in *Antennas and Propagation Society International Symposium, 1998. IEEE*, vol. 1, 1998, pp. 126–129 vol.1.

[5] J. Ilvonen, O. Kivekas, J. Holopainen, R. Valkonen, K. Rasilainen, and P. Vainikainen, "Mobile terminal antenna performance with the user's hand: Effect of antenna dimensioning and location," *Antennas and Wireless Propagation Letters, IEEE*, vol. 10, pp. 772–775, 2011.

[6] G. F. Pedersen, J. O. Nielsen, K. Olesen, and I. Z. Kovacs, "Measured variation in performance of handheld antennas for a large number of test persons," in *Vehicular Technology Conference, 1998. VTC 98. 48th IEEE*, vol. 1, May 1998, pp. 505–509 vol.1.

[7] A. Tatomirescu and G. F. Pedersen, "User body loss study for popular smartphones," in *2015 9th European Conference on Antennas and Propagation (EuCAP)*, May 2015, pp. 1–4.

[8] J. Krogerus, J. Toivanen, C. Icheln, and P. Vainikainen, "User effect on total radiated power and 3-d radiation pattern of mobile handsets," in *2006 First European Conference on Antennas and Propagation*, Nov 2006, pp. 1–6.

[9] ——, "Effect of the human body on total radiated power and the 3-d radiation pattern of mobile handsets," *IEEE Transactions on Instrumentation and Measurement*, vol. 56, no. 6, pp. 2375–2385, Dec 2007.

[10] F. C. Commission, "Fcc 96-326: Guidelines for evaluating the environmental effects of radio frequency radiation," Tech. Rep., 1996.

[11] B. S. Institution, *BS EN 50361:2001*. BSI, 2001.

[12] C. Certification, "Test plan for mobile station over the air performance—method of measurement for radiated rf power and receiver performance," 2008.

[13] C. C. Gordon, T. Churchill, C. E. Clauser, B. Bradtmiller, and J. T. McConville, "Anthropometric survey of us army personnel: methods and summary statistics 1988," DTIC Document, Tech. Rep., 1989.

[14] M. Pelosi, O. Franek, M. B. Knudsen, M. Christensen, and G. F. Pedersen, "A grip study for talk and data modes in mobile phones," *IEEE Transactions on Antennas and Propagation*, vol. 57, no. 4, pp. 856–865, April 2009.

[15] D. D. Sharrit, "Vector network analyzer with integral processor," Oct. 27 1987, uS Patent 4,703,433.

[16] D. Gesbert, M. Shafi, D. shan Shiu, P. J. Smith, and A. Naguib, "From theory to practice: an overview of mimo space-time coded wireless systems," *IEEE Journal on Selected Areas in Communications*, vol. 21, no. 3, pp. 281–302, Apr 2003.

[17] H. Li, Z. T. Miers, and B. K. Lau, "Design of orthogonal mimo handset antennas based on characteristic mode manipulation at frequency bands below 1 ghz," *IEEE Transactions on Antennas and Propagation*, vol. 62, no. 5, pp. 2756–2766, May 2014.

[18] J. . Nielsen, B. Yanakiev, S. C. D. Barrio, and G. F. Pedersen, "Channel statistics for mimo handsets in data mode," in *The 8th European Conference on Antennas and Propagation (EuCAP 2014)*, April 2014, pp. 2818–2822.

[19] F. Harrysson, A. Derneryd, and F. Tufvesson, "Evaluation of user hand and body impact on multiple antenna handset performance," in *2010 IEEE Antennas and Propagation Society International Symposium*, July 2010, pp. 1–4.

[20] P. Bahramzy, P. Olesen, P. Madsen, J. Bojer, S. C. D. Barrio, A. Tatomirescu, P. Bundgaard, A. S. M. III, and G. F. Pedersen, "A tunable rf front-end with narrowband antennas for mobile devices," *IEEE Transactions on Microwave Theory and Techniques*, vol. 63, no. 10, pp. 3300–3310, Oct 2015.

[21] E. Buskgaard, A. Tatomirescu, S. C. D. Barrio, P. Bahramzy, O. Franek, and G. F. Pedersen, "Simple front-end concept for the complex challenges of multi-band communications," in *2015 9th European Conference on Antennas and Propagation (EuCAP)*, May 2015, pp. 1–5.

[22] J. R. D. Luis, A. Morris, Q. Gu, and F. de Flaviis, "Tunable duplexing antenna system for wireless transceivers," *IEEE Transactions on Antennas and Propagation*, vol. 60, no. 11, pp. 5484–5487, Nov 2012.

[23] S. C. D. Barrio, A. Tatomirescu, G. F. Pedersen, and A. Morris, "Novel architecture for lte world-phones," *IEEE Antennas and Wireless Propagation Letters*, vol. 12, pp. 1676–1679, 2013.

[24] M. Gustafsson and B. L. G. Jonsson, "Antenna q and stored energy expressed in the fields, currents, and input impedance," *IEEE Transactions on Antennas and Propagation*, vol. 63, no. 1, pp. 240–249, Jan 2015.

[25] E. Buskgaard, A. Tatomirescu, S. C. D. Barrio, O. Franek, and G. F. Pedersen, "Effect of antenna bandwidth and placement on the robustness to user interaction," in *2014 International Workshop on Antenna Technology: Small Antennas, Novel EM Structures and Materials, and Applications (iWAT)*, March 2014, pp. 258–261.

[26] P. Bahramzy and G. F. Pedersen, "Detuning effect study of high-q mobile phone antennas," in *2015 9th European Conference on Antennas and Propagation (EuCAP)*, May 2015, pp. 1–4.

[27] P. Bahramzy, O. Jagielski, S. Svendsen, P. Olesen, and G. F. Pedersen, "Aspects of high-q tunable antennas and their deployment for 4g mobile communications [antenna applications corner]," *IEEE Antennas and Propagation Magazine*, vol. 58, no. 4, pp. 70–81, Aug 2016.

[28] E. F. Buskgaard, B. K. Krøyer, A. Tatomirescu, O. Franek, and G. F. Pedersen, "Tiny integrated network analyzer for noninvasive measurements of electrically small antennas," *IEEE Transactions on Microwave Theory and Techniques*, vol. 64, no. 1, pp. 279–288, Jan 2016.

[29] P. Bahramzy, O. Jagielski, S. Svendsen, and G. F. Pedersen, "Compact agile antenna concept utilizing reconfigurable front end for wireless communications," *IEEE Transactions on Antennas and Propagation*, vol. 62, no. 9, pp. 4554–4563, Sept 2014.

[30] V. I. Shalatonin, "Mobile phones and health: The key role of human body fluids in bioeffects of non-thermal em radiation," in *2008 18th International Crimean Conference - Microwave Telecommunication Technology*, Sept 2008, pp. 848–849.

[31] A. C. Silk, "Biological effects of microwave radiation-hot heads," in *IEE Seminar on Electromagnetic Assessment and Antenna Design Relating To Health Implications of Mobile Phones (Ref. No. 1999/043)*, 1999, pp. 4/1–4/4.

[32] J. C. Lin, "Malignant brain tumors from cellular mobile telephone radiation - [telecommunication health safety]," *IEEE Antennas and Propagation Magazine*, vol. 49, no. 1, pp. 212–214, Feb 2007.

[33] "Ieee standard for safety levels with respect to human exposure to radio frequency electromagnetic fields, 3 khz to 300 ghz," *IEEE Std C95.1-2005 (Revision of IEEE Std C95.1-1991)*, pp. 1–238, April 2006.

[34] "Ieee recommended practice for determining the peak spatial-average specific absorption rate (sar) in the human head from wireless communications devices: Measurement techniques," *IEEE Std 1528-2013 (Revision of IEEE Std 1528-2003)*, pp. 1–246, Sept 2013.

[35] B. Yanakiev, J. . Nielsen, and G. F. Pedersen, "Mimo channel measurements using optical links on small mobile terminals," in *2010 IEEE Antennas and Propagation Society International Symposium*, July 2010, pp. 1–4.

[36] M. Hirose, S. Kurokawa, and K. Komiyama, "Antenna measurements by one-path two-port calibration using radio-on-fiber extended port without power supply," *IEEE Transactions on Instrumentation and Measurement*, vol. 56, no. 2, pp. 397–400, April 2007.

[37] S. Kurokawa, M. Hirose, M. Ameya, and Y. Toba, "Antenna measurement by simple optical link system using radio on fiber technologies," in *2014 International Symposium on Electromagnetic Compatibility, Tokyo*, May 2014, pp. 670–673.

Part II

Papers

Paper A

Simple front-end concept for the complex challenges of multi-band communications

Emil Feldborg Buskgaard, Alexandru Tatomirescu, Samantha Caporal Del Barrio, Pevand Bahramzy, Ondrej Franek, Gert Frølund Pedersen

The paper has been published in the proceedings of
The 9th European Conference on Antennas and Propagation (EuCAP) 2015, pp. 1 - 5, 2015.

The layout has been revised.

Simple Front-End Concept for the Complex Challenges of Multi-Band Communications

Emil Buskgaard[1], Alexandru Tatomirescu[1], Samantha Caporal Del Barrio[1,2], Pevand Bahramzy[1,3], Ondrej Franek[1], Gert Frølund Pedersen[1]
[1]Section of Antennas, Propagation and radio Networking (APNet), Department of Electronic Systems, Faculty of Engineering and Science, Aalborg University, DK-9220, Aalborg, Denmark
{eb, ata, scdb, pb, of, gfp}@es.aau.dk
[2]WiSpry Inc., 20 Fairbanks, Suite198, Irvine, CA92618, USA
[3]Intel Mobile Communication Denmark Aps, Nørresundby, Denmark
pevand.bahramzy@intel.com

***Abstract*—This paper proposes a new architecture for mobile phone front-ends that dramatically reduces the complexity of multi-band smart phones. Traditional smart phone front-ends consist of many parallel transmit (Tx) and receive (Rx) chains each dedicated to a single band. The proposed architecture simplifies this by making few fully frequency tunable Tx and Rx chains that each cover multiple bands.**

Three implementations of antenna systems for the proposed architecture are shown and discussed. They all consist of separate Rx and Tx antennas with more than 25 dB of isolation in between. Combined with additional tunable Rx and Tx filters the Rx/Tx isolation reaches 50 dB which is comparable with the isolation achieved with commercially available static duplex filters.

Based on these antenna designs it is concluded that the proposed architecture is feasible for LTE phones and makes full coverage of all LTE bands realistic. Current 5G investigations show that the advantages of flexible front-ends will be even bigger as technology moves toward software defined radio.

***Index Terms*—4G mobile communication, Antenna efficiency, Antenna measurements, Reconfigurable antennas, Mobile antennas, Multifrequency antennas**

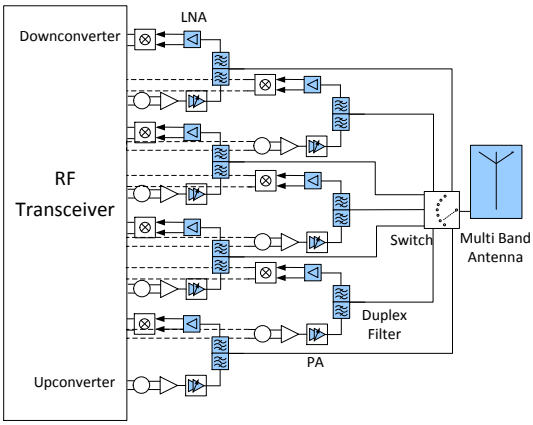

Fig. 1. Block diagram for a traditional RF front-end for a smartphone.

I. INTRODUCTION

THE trend in smart phones dictates slimmer phones with displays that cover as much of the front as possible. The antennas have to utilize the small parts of the phone that are outside the screen area. These areas also house speakers and connectors with metal parts. At the same time the requirement for bandwidth rises with every introduction of a new band to the 3GPP Long Term Evolution (LTE) standard [1].

The requirement for large bandwidth and small form factor has led to phone antennas with considerable losses [2]. Certain phone manufacturers are starting to make tunable antennas to optimize the antenna dynamically to the band of interest and thereby utilizing the limited volume of the antenna better [3]. This study takes this idea one step further.

In a traditional architecture as shown in Figure 1, there is one Tx and one Rx chain in the front end for each band. This architecture is expensive to scale as for every band an extra duplex filter and more switching, increasing the loss, must be added. Therefore, phones will often only support LTE in certain regions of the world and the manufacturers are forced to make separate band configurations for the same phone if they would like to sell it world wide.

In this study, the antenna is shrinked and a very narrow bandwidth is achieved with a large Q and acceptable losses. Hereby the antenna is not only band selective but channel selective. Such an antenna will only cover either the Rx channel or the Tx channel in an FDD system. By using separate antennas for Rx and Tx and tuning them to their respective frequencies a certain amount of Rx/Tx isolation is achieved. The hypothesis for this study is that this isolation, together with additional tunable filters, can provide the duplex isolation traditionally achieved with a duplex filter. By replacing this fixed frequency selective part of the RF chain a fully tunable front-end covering multiple bands can be realized.

In Section II the proposed architecture is explained. Section III analyses several antenna designs that have been developed specifically for the proposed architecture and shows measured results for each of them. Finally, Section IV draws the conclusions.

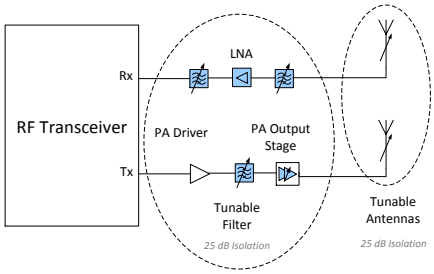

Fig. 2. Conceptual implementation of the proposed architecture for a front-end with separate Rx and Tx chain that can be tuned to any band of interest.

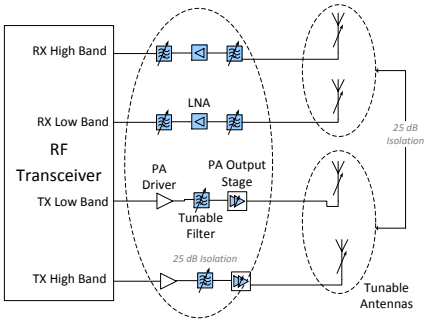

Fig. 3. Proposed architecture for a flexible front-end consisting of two Rx/Tx chains covering high and low bands respectively.

II. ARCHITECTURE

The proposed architecture only contains tunable frequency selective components and is thus band-independent. Hereby it is able to cover all bands in a large frequency range with one Tx and one Rx chain. This dramatically cuts cost and complexity and enables an architecture as shown in Figure 2. At the time of writing the maximum number of bands supported by one phone is 20 [4]. With the proposed architecture, all 40 LTE bands could be supported with only 1 simple Rx/Tx chain.

To limit the requirements for tunability of the front-end, the frequency range is divided into two bands as shown in Figure 3. This limits the fractional bandwidth from 127.3% for all bands from 600 - 2700 MHz to 46.2% for low band (LB: 600 MHz - 960 MHz) and 45.5% for high band (HB: 1700 MHz - 2700 MHz).

Typical link budget calculations indicate that 50 dB of Rx to Tx isolation is required to operate a phone in FDD mode. This is in line with the isolation of 40 - 60 dB achieved by commercially available duplex filters [5]. Tunable filters are available with isolation up to 30 dB [6]. Based on this it is assumed that 25 dB of isolation is required in addition to the tunable filter isolation to enable FDD operation.

This isolation is proposed to be achieved by separating the Rx and Tx on different narrow band antennas. The high selectivity of the antennas will - in combination with the spatial separations of the Rx and Tx antennas - enable the required isolation between Rx and Tx even at very low frequencies e.g. down to 600 MHz. It is chosen to aim for at least 10 MHz of instantaneous bandwidth across the full tuning range of the antenna. The following section will show different antenna implementations developed specifically for this architecture.

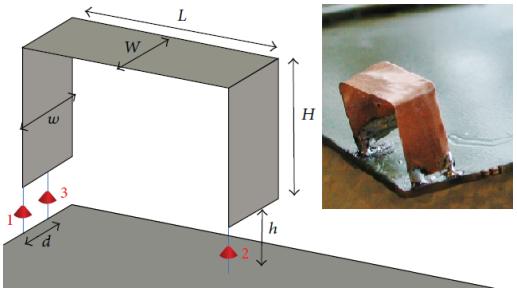

Fig. 4. Antenna design for investigation of wide band tuning of a small element [7]. In the top corner a picture of the actual measured antenna.

TABLE I
HIGH BAND AND LOW BAND ANTENNA DIMENSIONS [MM] OF DESIGN SHOWN IN FIGURE 4.

Band	L	H	W	w	h	d
High band (HB)	10	5	5	5	≈0	4
Low band (LB)	10	10	5	5	≈0	4

III. IMPLEMENTATIONS

Specific to the architecture described in the previous section, different antennas can be designed. This section describes a variety of antenna systems that can achieve 25 dB of Rx/Tx isolation while delivering the bandwidth required by the Long Term Evolution (LTE) standard release 12 [1]. All the prototypes described in this section have been mounted on generic ground planes of 120 mm × 54 mm and measured.

A. Widely tuned element

First a test has been made to examine the assumption that using one very small antenna and tuning it all the way from 700 MHz to 2700 MHz will have too many draw backs [7]. The design is shown in Figure 4 and consists of a metal arc placed over the ground plane. It is a top-loaded planar inverted-F antenna (PIFA) with grounding and feed along one end and a tunable capacitor at the opposite end. The dimensions are listed in Table I.

The tunable capacitor, C_1, has a minimum capacitance (C_{min}) of 1 pF and a maximum capacitance (C_{max}) of 4.875 pF and is placed in series with a 0.6 pF capacitor for the HB test as shown in Figure 5A). By sweeping the capacitance value of the tunable capacitor the frequency spectrum from 2400 to 2700 MHz can be covered as seen in Figure 6. Figure 7 shows the associated efficiencies are acceptable at a level between -2 and -3 dB.

The same antenna topology is afterwards tuned to a low frequency range from 700 to 940 MHz as can be seen from

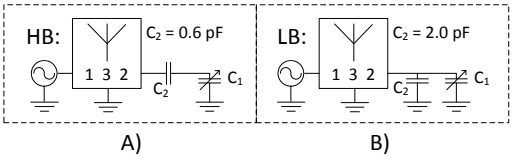

Fig. 5. Schematics for the antenna circuitry for high band (A) and low band (B) for wide band tuning experiment [7].

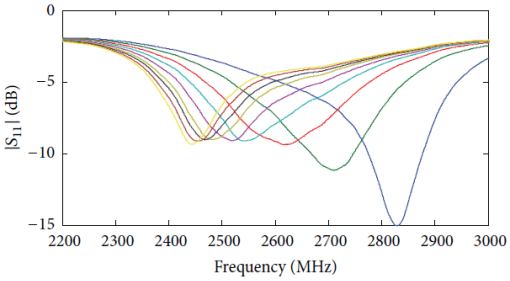

Fig. 6. Measured return loss of the antenna of [7], shown in Figure 4, when tuned to 2400 - 2700 MHz.

Figure 8. Two modifications are made; The height of the antenna element is increased from 5 to 10 mm to keep an acceptable bandwidth and instead of the fixed series capacitor a parallel capacitor of 2 pF is used as depicted in Figure 5B). Figure 9 shows the losses across the frequency range and here it is clear that the excessive tuning has hurt the performance. The losses exceed 10 dB at the low end of the spectrum. This confirms the assumption that splitting the frequency range into a low band (700 - 960 MHz) and a high band (1700 - 2700 MHz) is the better approach.

B. Full Rx/Tx system for high band

After concluding that one antenna covering all bands will have too low efficiency in the low band the following solutions will utilize separate high band and low band antenna elements. The first implementation is a separate Rx/Tx antenna system for the high band only described in detail in [8]. Each antenna

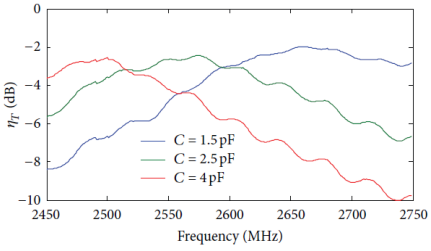

Fig. 7. Measured losses of the antenna of [7], shown in Figure 4, when tuned to 2400 - 2700 MHz.

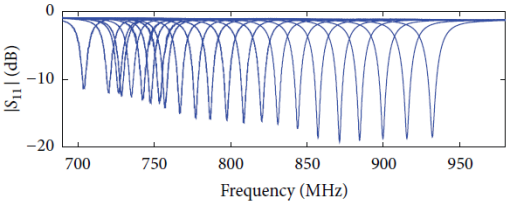

Fig. 8. Measured return loss of the antenna of [7], shown in Figure 4, when tuned to 700 - 940 MHz.

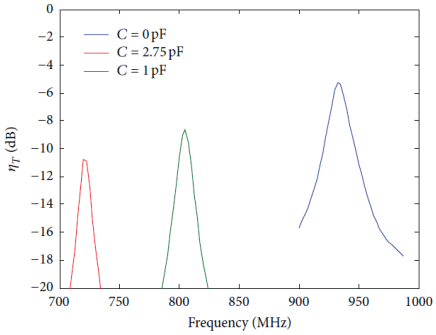

Fig. 9. Measured losses of the antenna of [7], shown in Figure 4, when tuned to 700 - 940 MHz.

element consists of 2 coupled strips mounted at one end of the ground plane as shown in Figure 10. The monopoles are designed with a tunable capacitor on the arm that enables tuning. A sketch of the elements can be seen in Figure 11.

Figure 12 shows the S-parameters for the measured prototype. It can be seen that the isolation between the antennas always is better than 25 dB as specified. The efficiency of the antenna is between -2.0 and -6.7 dB across the tuning range. The efficiency is best at high frequencies and deteriorates as the capacitance is increased. The decrease of efficiency is mainly due to thermal losses in the capacitor but also affected

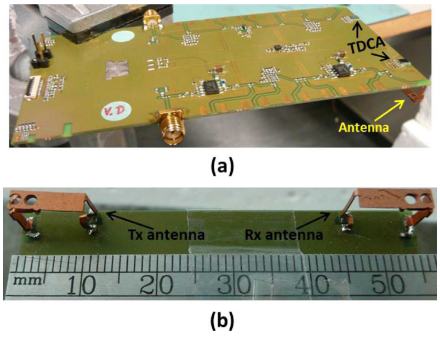

Fig. 10. Physical implementation of the antenna system used for measurements in [8]. (a) shows the complete mock-up, (b) shows a magnified view of the antennas.

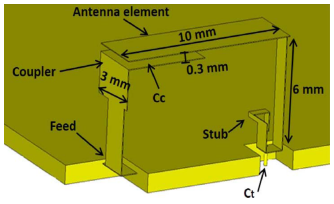

Fig. 11. 3D drawing of the antenna element of [8].

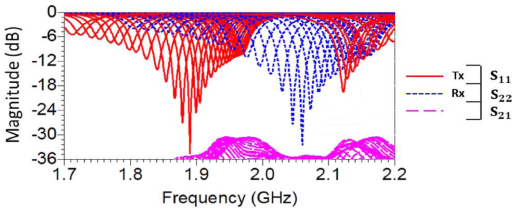

Fig. 12. Measured S-parameters of the antenna system shown in Figure 11 as reported in [8].

by a worsening of the match.

C. Full Rx/Tx system for both high and low band

With the second design showing promising results for the high band, a third design is made that covers both high band and low band with separate elements. A detailed description is available in [9]. In Figure 13 the design of one element is shown with dimensions and values for the matching components. A similar element will be placed on the side of the phone to achieve orthogonality of the ground currents. This is important to achieve the lowest possible coupling. As can be seen the element has a single feed for HB and LB but separate tuning.

As seen from Figure 14 and 15, the antennas are covering both high band and low band with at least the 25 dB of isolation required. The instantaneous bandwidth is 14 MHz at the high end of the tuning range which is fine but it drops to 6 MHz at 700 MHz and 5 MHz at 600 MHz. This is not

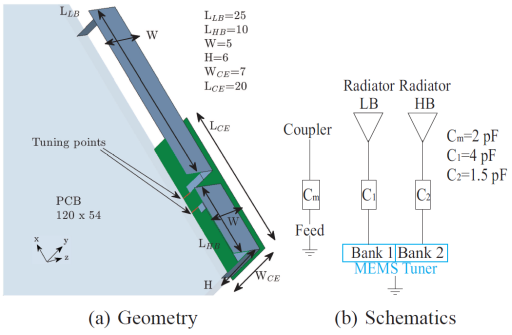

(a) Geometry (b) Schematics

Fig. 13. Antenna design for a complete system of both high and low band antennas [9]. All dimensions are in mm

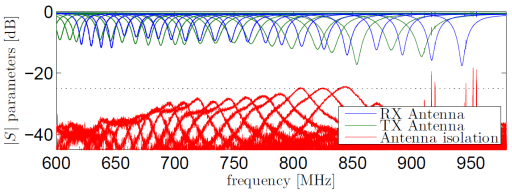

Fig. 14. Measured S-parameters of the low band antenna of [9], shown in Figure 13, when tuned to 600 - 940 MHz.

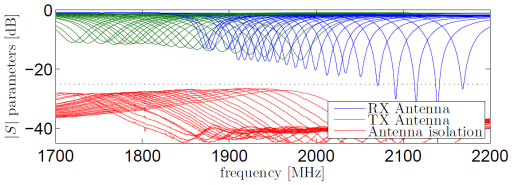

Fig. 15. Measured S-parameters of the high band antenna of [9], shown in Figure 13, when tuned to 1700 - 2200 MHz.

in line with specifications but can still be used for LTE for up to 5 MHz wide channels. The total efficiencies are listed in Table II and show that the antennas have good performance all the way down to 700 MHz. At 600 MHz the efficiency has dropped to -7 dB which is still acceptable in comparison to commercially available phones [2], [10].

TABLE II
MEASURED η_T OF THE TX ANTENNAS OF THE ANTENNA SYSTEM DESCRIBED IN [9] AND SHOWN IN FIGURE 13.

Freq [MHz]	1980	1710	900	800	700	600
η_T **[dB]**	-3	-4	-3	-4	-5	-7

This final design is thus directly feasible for full high and low band operation with only two RF chains. This is a clear verification of the hypothesis of this study.

IV. CONCLUSION

This study shows the necessity of rethinking the RF front-end architecture if true global LTE coverage should be made possible. Very few commercial phones currently support enough bands to offer some coverage across the globe and none are even close to covering all the bands defined for LTE.

The proposed architecture can change this. By utilizing tunable components for all frequency selective parts of the RF chain, every chain can cover many bands. With the concept proposed in this paper two Rx/Tx chains are used to cover the entire range from 600 - 960 MHz and 1700 - 2700 MHz. The implementations shown are proving that it is indeed possible to achieve the isolation needed between Rx and Tx antennas for a smart phone form factor.

In the future the need for flexible front-ends will only get larger. In Europe the work on the next generation wireless standard is spearheaded by the ”Mobile and wireless communications Enablers for Twenty-twenty (2020) Information Society” (METIS) project [11]. The METIS project foresees

disruptive changes to the mobile infrastructure based on the introduction of new technologies and applications. One keyword for the 5G standard is flexibility which is an inherent quality of the proposed solution.

REFERENCES

[1] "3rd generation partnership project; technical specification group radio access network; evolved universal terrestrial radio access (e-utra); user equipment (ue) radio transmission and reception (release 12)," The 3rd Generation Partnership Project (3GPP), http://www.3gpp.org/, Tech. Rep., 2014, 3GPP TS 36.101 V12.5.0.

[2] A. Tatomirescu and G. Pedersen, "Body-loss for popular thin smart phones," in *Antennas and Propagation (EuCAP), 2013 7th European Conference on*, April 2013, pp. 3754–3757.

[3] *nubia Adopts Cavendish Kinetics SmarTune Antenna Tuning Solution for its new Z7 LTE Smartphone*, Cavendish Kinetics, October 2014, Press Release. [Online]. Available: http://www.cavendish-kinetics.com/index.php/news-media/press-releases/towerjazz-and-cavendish-kinetics-collaborate-deliver-high-vo2/

[4] *Apple - iPhone 6 - Connectivity*, Apple Inc, October 2014, Homepage. [Online]. Available: https://www.apple.com/iphone-6/connectivity/

[5] *SAW Filters for Mobile Communications*, Murata Manufacturing co. ltd., May 2012, PDF Catalog. [Online]. Available: http://www.murata.com/~/media/webrenewal/support/library/catalog/products/filter/saw/p72e.ashx

[6] *WiSpry Application Note, Network Examples, Version 1.0*, WiSpry Inc, September 2014, Application Note. [Online]. Available: http://www.wispry.com/admin/nav_pdf/nav_pdf_30.pdf

[7] S. Del Barrio, A. Morris, and G. F. Pedersen, "Antenna miniaturization with mems tunable capacitors: Techniques and trade-offs," *Hindawi International Journal of Antennas and Propagation*, vol. 2014, no. 1, pp. 1 – 8, August 2014.

[8] P. Bahramzy, O. Jagielski, S. Svendsen, and G. F. Pedersen, "Compact agile antenna concept utilizing reconfigurable front end for wireless communications," *Antennas and Propagation, IEEE Transactions on*, vol. 62, no. 9, pp. 4554 – 4563, SEPTEMBER 2014.

[9] S. Caporal Del Barrio, A. Tatomirescu, G. Pedersen, and A. Morris, "Novel architecture for lte world-phones," *Antennas and Wireless Propagation Letters, IEEE*, vol. 12, pp. 1676–1679, 2013.

[10] S. Del Barrio and G. Pedersen, "Correlation evaluation on small lte handsets," in *Vehicular Technology Conference (VTC Fall), 2012 IEEE*, Sept 2012, pp. 1–4.

[11] A. Osseiran, V. Braun, T. Hidekazu, P. Marsch, H. Schotten, H. Tullberg, M. Uusitalo, and M. Schellman, "The foundation of the mobile and wireless communications system for 2020 and beyond: Challenges, enablers and technology solutions," in *Vehicular Technology Conference (VTC Spring), 2013 IEEE 77th*, June 2013, pp. 1–5.

Paper B

User effect on the MIMO performance of a dual antenna LTE handset

Emil Feldborg Buskgaard, Alexandru Tatomirescu, Samantha Caporal Del Barrio, Ondrej Franek, Gert Frølund Pedersen

The paper has been published in the proceedings of
The 8th European Conference on Antennas and Propagation (EuCAP) 2014,
pp. 2006 - 2009, 2014.

User Effect on the MIMO Performance of a Dual Antenna LTE Handset

Emil Buskgaard*, Alexandru Tatomirescu*, Samantha Caporal Del Barrio*, Ondrej Franek*,
Gert Frølund Pedersen*
*Section of Antennas, Propagation and radio Networking (APNet), Department of Electronic Systems,
Faculty of Engineering and Science, Aalborg University, DK-9220, Aalborg, Denmark
{eb, ata, scdb, of, gfp}@es.aau.dk

***Abstract*—This study focuses on the user influence on a MIMO antenna system in a smart phone form factor. The antenna system is designed to have a low coupling and correlation between its two antennas. The study is based on time-domain simulations of the antenna system in free space and with a head and hand phantom using a commercially available Finite Element Method solver. The MIMO parameters are evaluated with three different channel models.**

A static grip only gives one case of the user effect so the hand phantom is modified with a moving finger that is swept across the backplane of the phone. Based on the results of the study it is concluded that the placement of the index finger has a significant effect on the simulated antenna system. For certain finger placements the mismatch loss and absorption loss both change more than 5 dB.

Overall the antenna system shows good MIMO performance in free space but suffers under the influence of the user. Especially the diversity antenna is heavily detuned and gives a total efficiency of -19.1 dB worst case compared to -1.9 dB in free space. The branch power ratio is increased by the user while the envelope correlation is decreased by the user.

***Index Terms*—MIMO,**

I. INTRODUCTION

WITH the introduction of Long Term Evolution (LTE) Multiple Input Multiple Output (MIMO) has become a common requirement for mobile phones. The benefit in terms of throughput of MIMO can be huge for a well designed antenna system where the antennas are sufficiently decorrelated and isolated. If the correlation is too strong between the antennas the data streams are harder to separate and the throughput is reduced. For Signal to Noise Ratio (SNR) limited MIMO links the throughput is limited by the Branch Power Ratio (BPR) as well. In this case if one antenna is receiving significantly more power than the other then the weaker antenna link will have a lower SNR and thus not be able to support as high a data rate as the strong link.

The effect of the user has long been acknowledged as a major influence on mobile antenna performance [1]–[4]. It both absorbs power as well as detunes the center frequency of the antenna. Absorption loss is intrinsic to the interaction with a user. The absorption loss varies depending on the antenna type and user hand and head size and grip style. The absorption in the hand and head of the user will be beneficial for isolation between the MIMO antennas but the user may also compromise the orthogonality of the ground currents caused by the two antennas according to the characteristic mode theory [5], [6] causing the isolation to decrease.

This study looks at the correlation and coupling between two antennas in a Down-Link (DL) MIMO setup for LTE Band 13. The main antenna is covering both the Rx and the Tx frequencies while the diversity antenna only covers the Rx portion of Band 13. The designed MIMO antenna configuration is evaluated based on Computer Simulation Technology (CST) [7] simulations. For each configuration the free space performance is compared to the performance under influence of the CTIA Specific Anthropomorphic Mannequin (SAM) head phantom and the CTIA hand model for talk position [8]. Section II will specify the antenna design that has been developed for this study as well as the modeling of the user. In Section III the simulation procedure and the different channel models used for the MIMO parameters are described. Section IV presents and discusses the results while the conclusion of the study is formulated in Section V.

II. SIMULATION SETUP

All simulations are performed on a MIMO antenna system for LTE Band 13 in the presence of the CTIA SAM head and the CTIA hand. Band 13 is a very challenging LTE band since the frequency is low and the phone PCB therefore becomes electrically short. Fig. 1 shows the antenna system consisting of a ground plane (GND) with two folded monopole antennas. The antenna at the end of the GND is the main antenna covering all of Band 13 (746 - 787 MHz) while the side antenna is the diversity antenna only covering the RX band (746 - 756 MHz). Each antenna is matched with an inductor in parallel to the port. The antenna system is enclosed in a housing with sides made of 1 mm thick plastic and front and back made of 0.5 mm plastic. All dimensions of the antennas and housing are listed in Table I. This table also includes a list of materials and their parameters as well as the values of the parallel matching inductances.

To quantify the effect of the antenna placement on the immunity to the user the antenna system is simulated both with the main antenna at the top of the phone (close by the ear) and the diversity antenna on the side, Top-Side (TS), and at the bottom and side, Bottom-Side (BS). The antenna system is not changed between TS and BS but only rotated 180° inside the casing. This means that both the main and diversity antenna

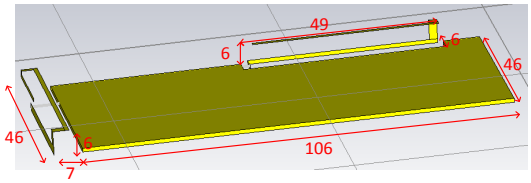

Fig. 1. Dimensions of the simulated PCB with MIMO antenna setup.

is changing position with respect to the user but the phone performance does not change in free space (FS)

The phone models are placed into a modified CTIA hand where the index finger has been replaced by a parameterized model that can be moved over the back plane of the phone. The dimensions of the parameterized finger are taken from [8]. The material is identical and all dimensions are kept in line with the CTIA specification. The angles of the bends in the finger are changed within the realistic movement of the finger. The finger tip is swept across the six positions shown on Fig. 2.

To get a realistic simulation of the losses in talk mode the influence of the head must also be included. This is done by adding a model of the CTIA specified SAM. It consists of an outer shell filled by a liquid that emulates the properties of the human head. The properties at the chosen frequency band are listed in Table I.

III. SIMULATION PROCEDURE

The simulations presented are done using the transient solver of CST. It utilizes the Finite Element Method (FEM) to simulate the response of the 3D structure to a short pulse that is exciting all frequencies of interest. A hexahedral mesh is chosen with minimum 20 mesh cells per wavelength.

First a baseline simulation is done for the antenna, ground plane and housing without the SAM phantom and CTIA hand. The dimensions of the antennas are adjusted to tune the antennas and values of the parallel inductors are adjusted to match the antennas. Then the head and hand are added and the position of the tip of the index finger is swept across the six positions shown on Fig. 2. For each position a simulation is done and the results are compared to the free space baseline. This is done to investigate the existence of sensitive spots on the ground plane, and their effect on antenna performance. Performance limitations due to the user interaction are more likely found by this procedure.

TABLE I
ANTENNA CONFIGURATION DIMENSIONS AND MATERIAL PROPERTIES

Antenna Dimensions [mm]:			
Name	**H**	**W**	**T**
Primary	7	46	6
Diversity	6	49	6
PCB	106	46	1
Housing	117	52	8

Material properties @ 751 MHz:			
Part	**Material**	ε_r	**tan** δ
Casing	Plastic	2.8	0.002
Hand	CTIA spec	31.8	0.421
Head shell	CTIA spec	3.5	0
Head fill	IEEE1528 liquid	41.8	0.504
Antennas	Copper	σ = 5.96e7 S/m	

Matching inductance parallel to feed:		
$\mathbf{L}_{Feed}$	Primary: 5.5 nH	Diversity: 3.0 nH

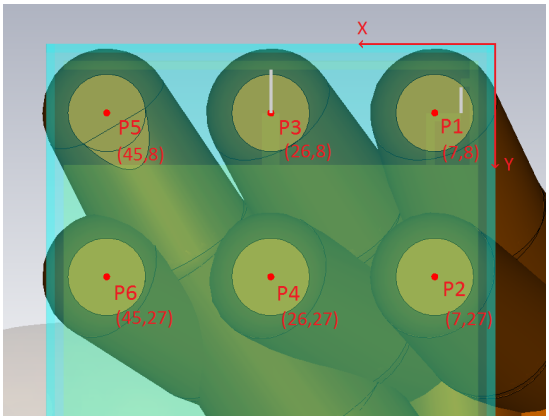

Fig. 2. Index finger positions used for simulations of hand effect. Coordinates are in mm from the top right corner of the phone. Finger tip is touching the backside of the phone in the light brown regions.

The results of the simulations are sets of S-parameters from the two antennas and antenna patterns for each antenna. From the antenna patterns, the envelope correlation and branch power ratio (BPR) between the antennas is calculated. The cross correlation is calculated for three different channel models:

Isotropic The isotropic channel model is the simplest and least realistic. It assumes a completely uniform power distribution from all directions. This gives the most optimistic result for correlation between the antenna patterns of the two antennas.

Gaussian The Gaussian channel model was introduced in [9] by Taga. Building on analysis of antennas moving around in a mobile communication environment, this model gives a statistical representation of the incident power distribution for an antenna. The model assumes equal probability of the power from all directions in the horizontal plane and a Gaussian distribution across elevation with maximum in the horizontal plane. It is a multi-path environment with cross polarization (XPD) of 1, and for vertical, V, and horizontal, H, polarizations the mean elevation, m, and standard deviation, σ, are:

$$\text{XPD} = 3 \text{ dB}$$
$$\text{m}_V = 0^\circ \quad \sigma_V = 40^\circ$$
$$\text{m}_H = 0^\circ \quad \sigma_H = 60^\circ$$

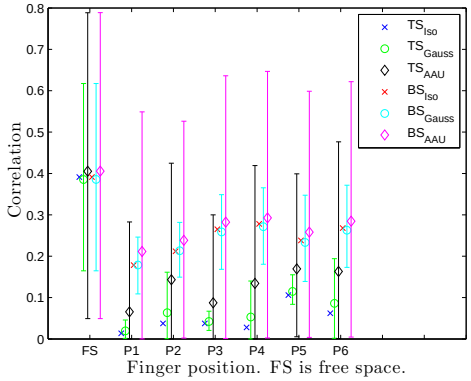

Fig. 3. Simulated correlation between main and diversity antenna at 751 MHz for Isotropic, Gaussian and AAU environment. TS is top-side antenna configuration while BS is bottom-side configuration.

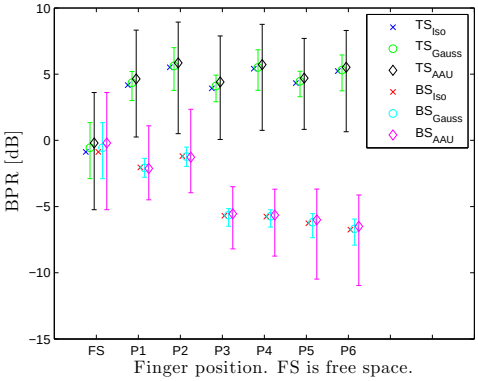

Fig. 4. Simulated BPR between main and diversity antenna at 751 MHz for Isotropic, Gaussian and AAU environment. TS is top-side antenna configuration while BS is bottom-side configuration.

AAU The AAU channel model was introduced in [10] as a realistic channel model for outdoor to indoor environments. The model is based on live measurements that showed that radio signals primarily enter a building through the windows. Therefore the model assumes that the majority of the power comes from one direction. [10] lists the parameters for the model based on experimental data. These values are used for the model in this paper as well.

IV. RESULTS

This paper focuses on the added information that the array of finger positions gives. To evaluate the added value of the finger position sweeping simulated values for both single antenna parameters as well as array parameters are presented. The parameters are presented for free space (FS) and for each of the six finger positions (P1 to P6) shown in Fig. 2. Results are presented for both the TS and BS antenna configuration described earlier.

Fig. 3 shows the correlation between the antennas. Data series are included for the three different channel models for both the TS and BS configuration. The antenna systems are rotated in 30° intervals on azimuth, elevation and orientation with respect to the incoming power distribution of the channel. For the Isotropic channel model the power distribution is completely uniform from all directions so spinning the phone yields the same result for all angles. Therefore the data series of the Isotropic model has only one value per finger position. For the Gaussian and AAU models there is a spread of the correlation across all orientations of the phone. Here, the minimum, mean and maximum values are all included on the graphs.

The antenna system is designed to have low correlation between the two antenna patterns and it achieves approximately 0.4 in FS as an average value. This is a good performance. The head and hand improves the correlation for all finger positions. The finger movement does not make a clear difference in the correlation values.

The finger position has a more clear effect on the BPR as seen in Fig. 4. The data series on this figure are generated and organized in the same way as on Fig. 3. Here the head and hand deteriorates the BPR by up to 10 dB. For TS the BPR is only mildly affected by the movement of the finger. There is a vague trend that the lower finger positions give worse BPR but it is not pronounced. For BS though the effect of the finger is noticeably different for P1 and P2 than for the rest. Here the proximity of the finger to the side antenna is helping to keep the branch power balanced giving a clear difference in performance on this parameter.

Table II shows the S-parameters of the two antenna configurations. Here especially the reflection coefficient of the top mounted antenna (S_{11} of TS) is showing a strong influence of the finger position. For the upper finger positions the top antenna is detuned more than for the lower. This is to be expected since the upper finger positions are on top of the antenna where as the lower positions are just below it. There is a trend in S_{22} for BS showing 1 dB higher reflection coefficient for P1 and P2. This extra detuning results in several dB's of additional reflection. This also affects S_{21} that improves due to the added mismatch loss of the side antenna. In the TS configuration the side antenna is heavily mismatched by the user as well but equally for all finger positions.

Certain S-parameters show clear dependencies on the finger position. This indicates that the finger position is important for the S-parameters as well. A model like the proposed with a movable index finger provides additional information about the user induced performance degradation compared to the standard CTIA hand.

In Table III the radiation and total efficiencies are listed for each of the antennas in each of the antenna systems. R1 and R2 are the radiation efficiencies and T1 and T2 are the total efficiencies for the main and diversity antennas respectively. The effect of the head and hand is large on these parameters.

TABLE II
S-PARAMETERS OF TOP AND BOTTOM MOUNTED MIMO ANTENNA SYSTEM WITH CTIA HAND AND HEAD AT 751 MHZ. DATA FOR 6 DIFFERENT POSITIONS OF THE INDEX FINGER ARE COMPARED TO THE DATA IN FREE SPACE. ANTENNA 1 IS TOP OR BOTTOM MOUNTED AND ANTENNA 2 IS SIDE MOUNTED.

	Antennas: Top/side			**Antennas: Bottom/side**		
	S_{11}	S_{22}	S_{21}	S_{11}	S_{22}	S_{21}
FS	-7.9	-8.2	-8.4	-7.9	-8.2	-8.4
P1	-2.4	-1.2	-22.7	-5.5	-1.1	-21.0
P2	-4.8	-1.2	-22.5	-5.5	-0.6	-22.9
P3	-2.0	-1.2	-22.8	-5.1	-1.8	-19.7
P4	-4.8	-1.2	-22.2	-5.2	-1.9	-19.2
P5	-1.5	-1.1	-22.6	-4.8	-2.6	-19.4
P6	-4.3	-1.1	-22.5	-5.0	-2.0	-18.5

TABLE III
RADIATION AND TOTAL EFFICIENCY OF TOP AND BOTTOM MOUNTED MIMO ANTENNA SYSTEM WITH CTIA HAND AND HEAD AT 751 MHZ. DATA FOR 6 DIFFERENT POSITIONS OF THE INDEX FINGER ARE COMPARED TO THE DATA IN FREE SPACE. ANTENNA 1 IS TOP OR BOTTOM MOUNTED AND ANTENNA 2 IS SIDE MOUNTED.

	Antennas: Top/side				**Antennas: Bottom/side**			
	R1	**R2**	**T1**	**T2**	**R1**	**R2**	**T1**	**T2**
FS	-0.2	-1.1	-1.0	-1.9	-0.2	-1.1	-1.0	-1.9
P1	-13.4	-9.2	-15.8	-14.8	-8.9	-10.9	-9.6	-17.0
P2	-14.1	-8.6	-14.7	-14.6	-8.6	-9.7	-9.0	-18.5
P3	-13.3	-9.3	-16.2	-14.9	-8.7	-14.4	-9.7	-18.5
P4	-14.3	-8.9	-14.9	-14.9	-8.6	-14.4	-9.6	-18.2
P5	-14.0	-9.6	-17.6	-15.5	-8.9	-15.2	-9.9	-18.8
P6	-14.0	-8.8	-14.6	-15.0	-8.7	-15.4	-9.7	-19.1

Again, the effect of the index finger is most visible for the side antenna in the BS configuration. Here R2 is 4 to 5 dB better for P1 and P2 than for the other finger positions. The difference is evened out in T2 because of the larger mismatch loss for P1 and P2. For TS, T1 is having a bit of variation between upper and lower finger positions which is also due to the difference in mismatch loss.

V. CONCLUSION

This paper has investigated the MIMO performance of a dual antenna system. The system is built from two antennas that are decoupled by placing them such that they excite different modes on the ground plane. The antenna system is encased in a plastic casing and tuned to LTE band 13 by adjusting the length of the antenna trace. The aim of the study is to quantify the spread of correlation and coupling between the antennas in the presence of the user. The phone is placed in talk position with a CTIA head and hand. The phone is simulated both with the main antenna pointing up and down.

This setup is simulated using CST. The user effect is simulated by using imported simulation models of the CTIA head and hand phantoms. The CTIA hand is refined with a parametric flexible model of the index finger. Six positions on the back plane of the phone are simulated.

The data shows that the MIMO performance is good in free space. The average values for both correlation and BPR are not affected by the channel model but the variation increases with the directivity of the channel model. For worst case orientations of the phone in the highly directional AAU channel model, the correlation becomes a bit too high, almost 0.8. In all other situations the correlation is between 0.0 and 0.6 which is estimated to be good enough for MIMO. When adding the head and hand of the user the coupling is reduced by more than 10 dB. The average BPR is around 0 dB in FS and increasing with head and hand to 5 dB for TS with worst case values in the AAU channel model reaching almost 10 dB. For BS the average BPR is close to 0 dB for P1 and P2 but more than 5 dB for all other finger positions. The worst case BPR for BS exceeds 10 dB. The primary antenna total efficiency is down to -17.6 dB with the head and hand from -1.0 dB in FS. The diversity antenna has a worst case total efficiency of -19.1 dB compared to -1.9 dB in FS.

The diversity antenna is detuned significantly in both the TS and BS configuration. S_{22} increases from -8.2 dB in FS to -1.1 dB worst case for TS and from -8.2 dB in FS to -0.6 worst case for BS with head and hand. The main antenna is less affected by the user but it does suffer up to 6.4 dB increase in S_{11} for TS when the finger is placed on top of the antenna.

It is clear that the finger position is affecting certain parameters of the antennas significantly. The BPR, radiation efficiency and mismatch are all dependent on finger position. Since the grip style of cell phone users does vary a lot it is an important addition to the CTIA model to include this variation. For instance the mismatch loss of the side antenna in the BS configuration varies by roughly 5 dB for across index finger positions. If adaptive matching should be designed for this antenna system then this could be important information for the requirements for the antenna tuner.

REFERENCES

[1] G. Pedersen, "Antennas for small mobile terminals," Ph.D. dissertation, Aalborg University, 2003.

[2] M. Pelosi, "Users influence mitigation for small terminal antenna systems: Ph.d. thesis," Ph.D. dissertation, Aalborg University, 2009.

[3] P. Eratuuli, P. Haapala, P. Aikio, and P. Vainikainen, "Measurements of internal handset antennas and diversity configurations with a phantom head," in *Antennas and Propagation Society International Symposium, 1998. IEEE*, vol. 1, 1998, pp. 126–129 vol.1.

[4] J. Ilvonen, O. Kivekas, J. Holopainen, R. Valkonen, K. Rasilainen, and P. Vainikainen, "Mobile terminal antenna performance with the user's hand: Effect of antenna dimensioning and location," *Antennas and Wireless Propagation Letters, IEEE*, vol. 10, pp. 772–775, 2011.

[5] R. F. Harrington and J. Mautz, "Theory of characteristic modes for conducting bodies," *Antennas and Propagation, IEEE Transactions on*, vol. 19, no. 5, pp. 622–628, 1971.

[6] R. Garbacz and R. Turpin, "A generalized expansion for radiated and scattered fields," *Antennas and Propagation, IEEE Transactions on*, vol. 19, no. 3, pp. 348–358, 1971.

[7] C. S. T. (CST). (2013, October) CST Official Website @ONLINE. [Online]. Available: http://www.cst.com

[8] CTIA, "Method of measurement for radiated RF power and receiver performance." CTIA, Tech. Rep., November 2012, CTIA Certification Test Plan for Mobile Station Over The Air Performance. rev. 3.2. [Online]. Available: http://http://www.ctia.org/

[9] T. Taga, "Analysis for mean effective gain of mobile antennas in land mobile radio environments," *Vehicular Technology, IEEE Transactions on*, vol. 39, no. 2, pp. 117 –131, May 1990.

[10] M. Knudsen and G. Pedersen, "Spherical outdoor to indoor power spectrum model at the mobile terminal," *Selected Areas in Communications, IEEE Journal on*, vol. 20, no. 6, pp. 1156 – 1169, Aug. 2002.

Paper C

Effect of antenna bandwidth and placement on the robustness to user interaction

Emil Feldborg Buskgaard, Alexandru Tatomirescu, Samantha Caporal Del Barrio, Ondrej Franek, Gert Frølund Pedersen

The paper has been published in the proceedings of the *International Workshop on Antenna Technology: "Small Antennas, Novel EM Structures and Materials, and Applications" (iWAT) 2014* , pp. 258 - 261, 2014.

Effect of Antenna Bandwidth and Placement on the Robustness to User Interaction

Emil Buskgaard*, Alexandru Tatomirescu*, Samantha Caporal Del Barrio*, Ondrej Franek*,
Gert Frølund Pedersen*
*Section of Antennas, Propagation and Radio Networking (APNet), Department of Electronic Systems,
Faculty of Engineering and Science, Aalborg University, DK-9220, Aalborg, Denmark
eb, ata, scdb, of, gfp@es.aau.dk

***Abstract*—Modern smart phones require antenna systems that can deal with an ever-growing number of bands. This study compares two different approaches to the coverage of large bandwidths: Wide-band (WB) antennas covering a whole band at once and tunable narrow-band (NB) antennas covering only one channel at a time but tunable to all channels within the band of interest. To investigate the effect of antenna placement the antennas are placed both at the top and the bottom of the phone. All antenna configurations are simulated in talk position with a head and hand included. The hand is constructed with a movable index finger and the index finger is swept at 6 positions on the backside of the phone. The study shows that WB antennas detune a lot more than NB antennas and that top-mounted antennas are experiencing more than 6 dB higher losses than bottom-mounted antennas. It is proposed to expand this study with more antenna types and placements as both of these parameters are known to influence the immunity to the user. It is also proposed to compare the simulation results to measurements to increase the confidence in the results.**

***Index Terms*—Tunable Antenna, Coupling Element, Propagation Losses, Electromagnetic reflection.**

I. INTRODUCTION

THE required bandwidth of mobile phone antennas is increasing with every new generation of mobile telephony. For the 2^{nd} generation (GSM/GPRS) only 4 bands were defined world-wide. With Long-Term Evolution (LTE) the number of bands has risen to 40, thereof 23 FDD bands [1]. The LTE bands are situated in the frequency range between 700 MHz and 2.69 GHz. To cover all of these bands one can either make the antenna wide band (WB) and cover all frequencies of interest simultaneously with multi-resonant matching [2]–[4] or make the antenna tunable and adjust it for the frequencies of interest [5]–[7]. By making the antenna tunable, the bandwidth requirement is significantly reduced meaning that a smaller element can be used. The reduced volume of narrow-band (NB) antennas is very attractive for handset manufacturers since a significant part of the handset volume is taken up by antennas. The purpose of this study is to investigate the robustness of such a NB antenna to the proximity of the hand and head of a user. A comparison is made to a similar type of antenna with a larger height and five times larger bandwidth.

The effect of the user has long been acknowledged as a major influence on mobile antenna performance. It both absorbs power as well as detunes the center frequency of the antenna. Absorption loss is intrinsic to the interaction with a user. The absorption loss varies depending on the antenna type and user hand and head size and grip style [8]–[11]. For an active antenna the mismatch can be reduced by retuning. This requires closed-loop operation based on measurements of the mismatch. Since this is adding complexity to the transceiver it should only be considered if the mismatch loss is significant. The main objective of this study is to quantify how severe the mismatch loss can get for a NB tunable antenna compared to a conventional WB antenna.

In this study four different antenna configurations are compared based on CST simulations. For each configuration the free space performance is compared to the performance under influence of the CTIA Specific Anthropomorphic Mannequin (SAM) head phantom and the CTIA hand model for talk position [12].

This article is based on transient simulations done in CST [13]. The simulated setup is described in Section II. In Section III a description of the simulation procedure is given while Section IV contains the results of the simulations. Section V concludes on the results and proposes possible future investigations.

II. SIMULATION SETUP

All simulations are performed on a WB and a NB antenna in the presence of the CTIA SAM head and the CTIA hand. A simple Inverted-F-Antenna (IFA) with a width of 48 mm and a thickness of 6 mm is designed. The bandwidth of the antenna is controlled by the height of the antenna. This design is chosen to keep the WB and NB antennas as similar as possible with respect to the distance to the CTIA hand and the SAM phantom to get the most comparable results. The total height of the ground plane (GND) and antenna is kept constant at 106 mm. This is enclosed in a housing with sides made of 1 mm thick plastic and front and back made of 0.5 mm plastic. All dimensions of the antennas and housing are listed in Table I. This table also includes a list of materials and their parameters.

To quantify the effect of the antenna placement on the immunity to the user both antennas are simulated both in the top of the phone (close by the ear) and in the bottom

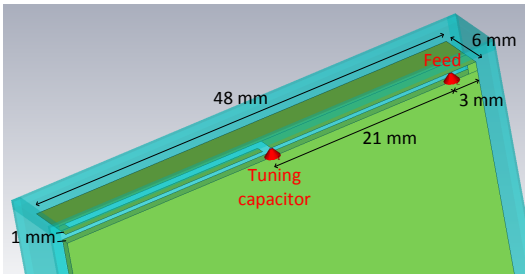

Fig. 1. Narrow-band antenna element design for the simulation. W = 48 mm, T = 6 mm, H = 1 mm.

of the phone. Both positions are likely to be used for an LTE phone since the requirement for Multiple-Input Multiple-Output (MIMO) means that at least two antennas must be fitted inside the volume of the phone. This means that a total of four configurations were simulated. The naming can be seen in Table I and is comprised of the antenna bandwidth and placement. Fig. 1 and 2 show the NB and WB antennas respectively.

The phone models are placed into a modified CTIA hand where the index finger has been replaced by a parameterized model that can be moved over the back plane of the phone. The dimensions of the parameterized finger are taken from [12]. This is of course an approximation of the index finger of the CTIA hand but since the material is the same and all dimensions are kept in line with the CTIA specification the results are deemed to be comparable to those with the default CTIA hand. The angles of the bends in the finger are changed within the realistic movement of the finger. The finger tip is swept across the six positions shown on Fig. 3.

To get a realistic simulation of the losses the influence of the head must also be included. This is done by adding a model of the CTIA specified SAM. This consists of an outer shell filled by a liquid that emulates the properties of the human head.

TABLE I
ANTENNA ELEMENT DIMENSIONS, MATERIAL PROPERTIES AND NAMING

Antenna Dimensions [mm]:			
Name	**H**	**W**	**T**
NBTM & NBBM	1	48	6
WBTM & WBBM	12	48	6
Housing	110	52	8
Material properties @ 751 MHz:			
Part	**Material**	ε_r	**tan** δ
Casing	Plastic	2.8	0.002
Hand	CTIA spec	31.8	0.421
Head shell	CTIA spec	3.5	0
Head fill	IEEE1528 liquid	41.8	0.504
Antennas	Copper	σ = 5.96e7 S/m	
NBTM & WBTM are top mounted			
NBBM & WBBM are bottom mounted			

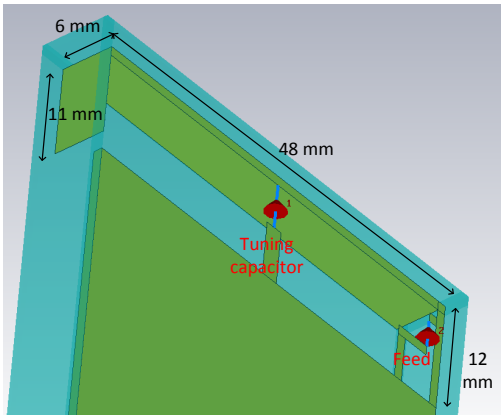

Fig. 2. Wide-band antenna element design for the simulation. W = 48 mm, T = 6 mm, H = 12 mm.

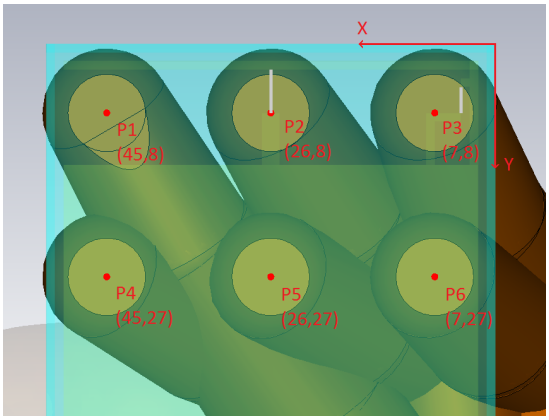

Fig. 3. Index finger positions used for simulations of hand effect. Coordinates are in mm from the top right corner of the phone. Finger tip is touching the backside of the phone in the light brown regions.

The properties are listed in Table I. The complete simulation setup can be seen in Fig. 4.

III. SIMULATION METHODOLOGY

The simulations presented are done using the transient solver of CST. This is utilizing the Finite Element Method (FEM) to simulate the response of the 3D structure to a short pulse that is exciting all frequencies of interest. For these simulations the frequency range is set to 0 - 3 GHz.

First a baseline simulation is done for the antenna, GND and housing without the SAM phantom and CTIA hand. The tuning capacitor on the antenna is adjusted to optimize S11 of the antenna at 751 MHz which is the center frequency of the down-link in LTE band 13. Then the head and hand are added and the position of the tip of the index finger is swept

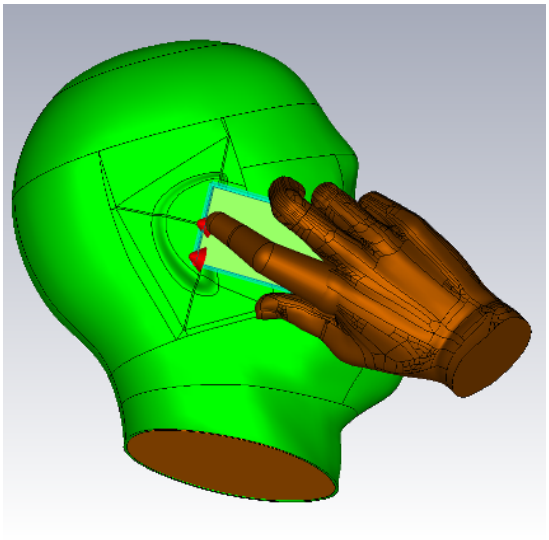

Fig. 4. Full simulation setup including phone, CTIA SAM head and CTIA hand with parameterized index finger.

across the six positions shown on Fig. 3. For each position a simulation is done and the results are compared to the free space baseline.

IV. SIMULATION RESULTS

The four different antenna configurations have been specified and simulated as described in the last two sections. Based on the results for the 6 different finger positions, Fig. 5 through 8 have been created. All charts are showing the maximum, minimum and average value based on the 6 finger positions. The results are both shown graphically and in the tables below the graphs for numerical accuracy.

Fig. 5 shows the detuning of the antennas calculated as the shift in frequency of the minimum of S_{11}. The frequency detuning is about 10 times worse for the WB antennas where frequency offsets in the order of 40 - 100 MHz are seen. The top mounted antennas experience about twice as much detuning and a lot more variation in detuning than the bottom mounted antennas.

Fig. 6 shows the mismatch loss calculated as the difference between the radiation efficiency and the total efficiency. The mismatch loss is 1 - 2 dB worse for the WB antennas due to the larger detuning. Losses of up to 4.5 dB are registered for the WBTM antenna. The mounting position has a large influence on the variation in mismatch loss with the top-mounted antennas being more sensitive to the movement of the index finger.

Fig. 7 shows the absorption loss calculated as the difference between the radiation efficiency with head and hand and the radiation efficiency with only the casing. The absorption loss is about 2 dB worse for WB than for NB antennas. For the

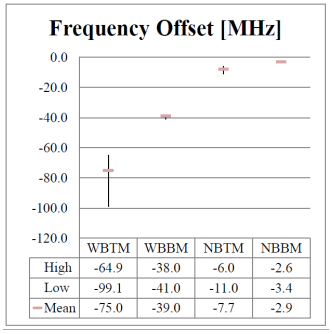

	WBTM	WBBM	NBTM	NBBM
High	-64.9	-38.0	-6.0	-2.6
Low	-99.1	-41.0	-11.0	-3.4
Mean	-75.0	-39.0	-7.7	-2.9

Fig. 5. Frequency detuning of the four antenna configurations.

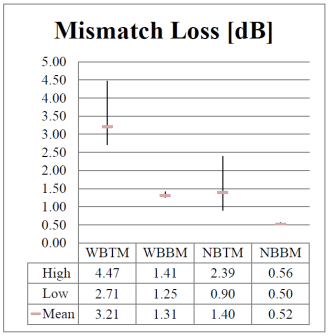

	WBTM	WBBM	NBTM	NBBM
High	4.47	1.41	2.39	0.56
Low	2.71	1.25	0.90	0.50
Mean	3.21	1.31	1.40	0.52

Fig. 6. Mismatch loss of the four antenna configurations.

WB antennas the loss including only the casing is 0.07 dB. This is not realistic as the copper itself will have some loss so it can be concluded that not all losses are modeled correctly. For the NB antennas the loss including only the casing is 2.25 dB. This shows that a lot more of the radiated fields are absorbed in the phone casing. This can explain why less power is absorbed in the head and hand compared to the WB antennas. The placement has an influence of 3 - 5.5 dB.

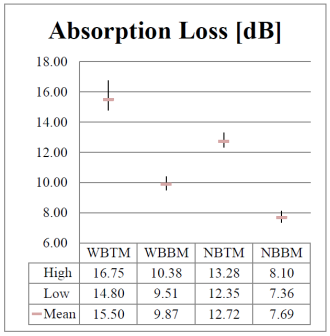

	WBTM	WBBM	NBTM	NBBM
High	16.75	10.38	13.28	8.10
Low	14.80	9.51	12.35	7.36
Mean	15.50	9.87	12.72	7.69

Fig. 7. Absorption loss of the four antenna configurations.

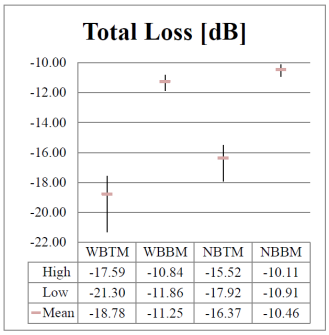

Fig. 8. Total loss of the four antenna configurations.

The total loss is shown in Fig. 8. Here it is evident that the mounting position of the antenna has a lot larger influence than the bandwidth of the antenna. The total loss is about 18 dB for top-mounted and 11 dB for bottom-mounted antennas and slightly worse for WB than for NB antennas.

V. CONCLUSION

This paper has investigated the degradation of the antenna performance due to the interaction with a user's hand and head. It has been demonstrated that the total loss of a NB and a WB antennas are comparable, however worse in the case of the WB antenna. It has also been seen that the placement of the antenna (top or bottom) is the most significant parameter. Both NB and WB antennas are predominantly suffering from absorption loss in proximity to the user. The antenna configurations with top mounted antenna are suffering more than 6 dB more total losses than with top mounted antenna.

Detuning is about a factor of ten worse for WB antennas than for NB antennas. Even with the larger bandwidth the WB antennas are suffering from larger mismatch losses than NB antennas. This means that for the WBTM antenna of this study there would be a benefit in implementing closed-loop antenna tuning. For bottom-mounted antennas the influence of the head and the hand is half that of the top-mounted antennas. It is however likely that a user with a different grip style could detune the antenna more for the bottom-mounted position as well. The influence of the movement of the index finger is much stronger for the top mounted antenna which makes sense since the movements are happening at the top end of the phone.

For modern smart phones the antenna system must support a multitude of standards of which some require MIMO meaning that it is not possible to avoid top mounted antennas. For the top mounted antenna the moving of the index finger is providing more realistic insight into the change in mismatch and absorption that the phone will experience than the static CTIA grip.

The conclusion of this study is that for the chosen antenna configurations there is 0.5 to 4.5 dB to gain by retuning the antenna to account for the user influence. The biggest losses are due to absorption in the users head and hand. It is furthermore concluded that the detuning is much more severe for the WB antenna of this study.

Further investigations include extending the study to more antenna types and placements as well as to verify the simulation results with measurements. Since the user effect is known to vary for different antenna types it is necessary to investigate their immunity to the moving index finger. Also side-placed antennas are often used and should therefore be examined with respect to the effect of the moving finger. Measurements should be done to get experimental data for the user effect and to compare with the simulations.

REFERENCES

[1] 3GPP, "LTE; evolved universal terrestrial radio access (E-UTRA); user equipment (UE) radio transmission and reception," 3GPP, Tech. Rep. 3GPP TS 36.101 version 12.1.0, September 2013.

[2] R. Valkonen, J. Ilvonen, C. Icheln, and P. Vainikainen, "Inherently non-resonant multi-band mobile terminal antenna," *Electronics Letters*, vol. 49, no. 1, pp. 11–13, 2013.

[3] F. Sonnerat, R. Pilard, F. Gianesello, F. Le Pennec, C. Person, and D. Gloria, "Innovative lds antenna for 4g applications," in *Antennas and Propagation (EuCAP), 2013 7th European Conference on*, 2013, pp. 2773–2776.

[4] Y.-L. Ban, C.-L. Liu, J.-W. Li, and R. Li, "Small-size wideband monopole with distributed inductive strip for seven-band wwan/lte mobile phone," *Antennas and Wireless Propagation Letters, IEEE*, vol. 12, pp. 7–10, 2013.

[5] F. G. Farrar, S. T. Hayes, D. H. Schaubert, and A. R. Sindoris, "Frequency-agile, polarization diverse microstrip antennas and frequency scanned arrays," U.S. Patent US4 367 474 A, January, 1983.

[6] K. Boyle and P. Steeneken, "A five-band reconfigurable pifa for mobile phones," *Antennas and Propagation, IEEE Transactions on*, vol. 55, no. 11, pp. 3300–3309, 2007.

[7] L. Huang and P. Russer, "Electrically tunable antenna design procedure for mobile applications," *Microwave Theory and Techniques, IEEE Transactions on*, vol. 56, no. 12, pp. 2789–2797, 2008.

[8] G. Pedersen, "Antennas for small mobile terminals," Ph.D. dissertation, Aalborg University, 2003.

[9] M. Pelosi, "Users influence mitigation for small terminal antenna systems: Ph.d. thesis," Ph.D. dissertation, Aalborg University, 2009.

[10] P. Eratuuli, P. Haapala, P. Aikio, and P. Vainikainen, "Measurements of internal handset antennas and diversity configurations with a phantom head," in *Antennas and Propagation Society International Symposium, 1998. IEEE*, vol. 1, 1998, pp. 126–129 vol.1.

[11] J. Ilvonen, O. Kivekas, J. Holopainen, R. Valkonen, K. Rasilainen, and P. Vainikainen, "Mobile terminal antenna performance with the user's hand: Effect of antenna dimensioning and location," *Antennas and Wireless Propagation Letters, IEEE*, vol. 10, pp. 772–775, 2011.

[12] CTIA, "Method of measurement for radiated RF power and receiver performance." CTIA, Tech. Rep., November 2012, CTIA Certification Test Plan for Mobile Station Over The Air Performance. rev. 3.2. [Online]. Available: http://http://www.ctia.org/

[13] C. S. T. (CST). (2013) CST Official Website @ONLINE. [Online]. Available: http://www.cst.com

Paper D

Tiny Integrated Network Analyzer for Noninvasive Measurements of Electrically Small Antennas

Emil Feldborg Buskgaard, Ben K. Krøyer, Alexandru Tatomirescu, Ondrej Franek, Gert Frølund Pedersen

The paper has been published in the
IEEE Transactions on Microwave Theory and Techniques, 2016, Volume: 64, Issue: 1, pp. 279 - 288, 2016.

Tiny Integrated Network Analyzer for Non-Invasive Measurements of Electrically Small Antennas

Emil F. Buskgaard, Ben K. Krøyer, Alexandru Tatomirescu, Ondřej Franek, Gert Frølund Pedersen

***Abstract*— Antenna mismatch and crosstalk are recurring issues in telecommunications. For electrically small antenna systems these are very hard to measure without affecting the radiation performance of the system and, consequently, the measurement itself. Electrically small antennas are found in many applications ranging from consumer electronics to industrial systems. We propose a radically new approach to characterize crosstalk and mismatch based on vector network analysis. By miniaturizing the network analyzer it can be integrated in the system under test eliminating the need for cables leaving the system. The tiny integrated network analyzer (TINA) is a stand-alone Arduino based measurement system utilizing the transmit signal of the system under test as its reference. It features a power meter with triggering ability, on-board memory, USB and easy extendibility with general purpose I/O. The accuracy and repeatability of the proposed system is documented through the repeatability of the calibration. To showcase the capabilities of the system, a measurement is done on a modified smart phone with the system inside. These early results show great promise for miniaturized network analysis. With the advances in software defined radio we can expect much more flexible and advanced integrated network analyzers in the coming years.**

***Index Terms*—Measurement techniques, Electrically-small antennas, Vector network analysis, Antenna measurements, MIMO, Calibration**

I. INTRODUCTION

THE advent of the Internet of things (IoT) brings a situation where a great number of various small devices are wirelessly connected in very diverse environments. Securing good radio performance for these networks is paramount as a unstable connection to a sensor could be problematic for i.e., the control of an industrial process or suboptimal performance of a battery powered device will decrease the battery life.

For many wireless systems the electrical size of the system is often much smaller than half the wavelength of the communication frequency. This means that their antennas are electrically small [1], [2]. Measurements on electrically small antennas (ESA) are challenging due to the high risk of interfering with the device under test (DUT) [3], [4]. Any metallic structure will couple to the antenna and change both the radiation pattern and the matching of the antenna. Furthermore these applications often have several antennas that are required to be decoupled and they often operate in highly dynamic environments where metallic objects or parts of a user's body enter the near field of the antennas.

All authors are with Section of Antennas, Propagation and Radio Networking (APNet), Department of Electronic Systems, Faculty of Engineering and Science, Aalborg University, DK-9220, Aalborg, Denmark ({eb, bk, ata, of, gfp}@es.aau.dk)

Accurate measurements of the coupling and reflection of electrically small antennas can help engineers to acquire vital information needed to create robust antenna systems. Such measurements can be used to verify that antenna systems can handle the mismatch that they will encounter during operation or to gauge the mismatch during operation for actively tuned antennas [5]–[8]. Current measurement techniques are not fit for electrically small antennas. The common approach is to measure the antenna impedance and coupling as S-parameters using a vector network analyzer (VNA). It relies on a VNA attached to the DUT by cables or optical fibers [9], [10]. When using coaxial cables, the cable will perturb the electrical fields close to the DUT [11]. By using an optical link this is prevented but also this approach has drawbacks. The authors are not aware of any commercial optical two-way link that is capable of measuring S-parameters and the implementations found are all encased in big metallic boxes.

Smaller VNA's exist on the market today. The miniVNA Tiny from mini Radio Solutions has a good frequency range of 1 MHz to 3 GHz. It is however still very big (66 x 66 x 28 mm) compared to the size of a phone or a tablet and it needs a USB connection to a PC to function. It is thus not truly wireless. [12] is another small USB connected VNA but it is even bigger and only reaches 1.3 GHz which is not enough for many modern wireless devices. All current VNA based options are thus not suitable for electrically small antenna systems at least if the frequency exceeds 1 GHz.

The proposed solution is to design a VNA that is small compared to the size of the DUT and can be integrated into the DUT. In this way the antenna S-parameters can be measured with minimal interference to the DUT. This new class of measurement equipment is dubbed the tiny integrated network analyzer, TINA. Obviously, a system that is reduced this much in size will not perform at the level of a full size VNA. It is believed that the most interesting insights to be gained from this new device are on the uncabled reflection of and coupling between ESA's, both in free space but particularly in proximity to users. For many applications, these figures are mostly interesting when their performance is bad meaning reflections higher than -6 dB or coupling higher than -10 dB. It is therefore not necessary to have a large dynamic range.

Although TINA as a class of measurement equipment serves a wide range of applications, a mobile phone is chosen to demonstrate the advantages of TINA. Performance of mobile phone antennas has been the subject of much discussion recently. Recent studies show that phone antennas in current smart phones are performing poorly both in free space and in the presence of the user [13].

The aim of the proof of concept is to measure the reflection of the main antenna and coupling between main and diversity antennas of the mobile phone (iPhone 5) during a live network call. During the call a test person will handle the phone in a natural fashion to replicate the user interaction occurring during a call or while browsing. It is important that the phone appears fully unchanged from the outside to enable the user to handle the phone naturally. To achieve this a smaller battery has been adapted to the phone to leave space in the phones battery compartment for the module to fit. It is thus fully embedded and no visible changes are made to the phone. For this proof of concept, the most important requirements are:

- The phone must be fully functional with original software and no noticeable change in performance.
- The phones appearance must be unchanged. This enables the most natural grip on the phone during the call giving the most realistic data possible.
- TINA must be able to sample both reflection and coupling of the antennas fast enough to analyze the changes in antenna performance induced by the user. 10 samples per second is believed to be fast enough.
- The system must be able to run for at least 30 minutes in a call. The battery must be large enough to power both the phone and TINA and the memory of TINA must be large enough to store the measurement data for 30 minutes of continuous measurements.

This article describes TINA and the first measurements made with it. In Section II the concept and implementation of the measurement setup are described, Section III shows the results of the calibration and the first measurement campaign conducted on the first phone with TINA embedded. Section IV discusses the accuracy of the calibration and the findings of the user study. Finally Section V concludes the study and presents the next steps.

II. METHODOLOGY

This section describes TINA as well as the other modifications that are made to the phone to enable the integration of TINA. Many modifications are necessary to achieve full integration of the module into the phone.

To minimize the size of TINA it has to be designed specifically for the application. TINA needs less dedicated circuitry if it can reuse the power supply, RF signal or digital processing of the DUT. In the case of a mobile phone a lot of options exist to use existing circuitry. The RF signal can be used as the reference of TINA if the phone is forced to operate in GSM mode. The GSM standard has a much lower power range (5 to 33 dBm in low band (LB) and 0 - 30 dBm in high band (HB)) than more recent standards lowering the requirement on dynamic range for TINA. Additional benefits of GSM is the time division duplexing (TDD) that can be used for timing of the measurements and constant envelope that due to the flat power level does not add to the dynamic range requirements for TINA.

GSM has a couple of negative features from the perspective of TINA. First of all GSM employs discontinuous transmission (DTX) meaning that the transmitter of the phone will not transmit a burst if there is nothing to transmit. This is done to decrease the interference to other GSM users. To avoid bursts from being omitted, it is thus necessary to apply a signal to the microphone of the phone. As the microphone interface is digital, it is found to be very difficult to apply a signal directly into the microphone lines. Instead a small speaker from a hearing aid is inserted very close to the microphone of the phone and supplied with tones generated by TINA microprocessor. An additional problem is frequency hopping. No complete solution is found for this issue as TINA has no ability to gauge the frequency of the transmit (Tx) signal. The spread in Tx frequencies is thus seen as a source of uncertainty to the results.

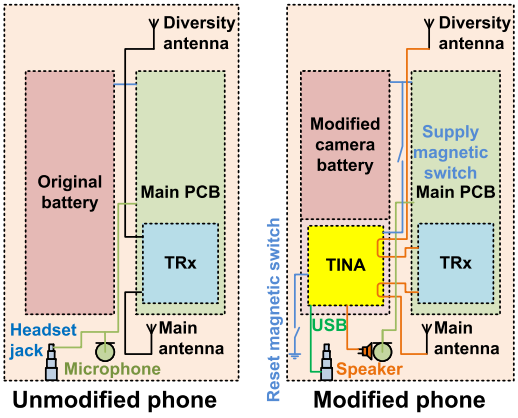

Fig. 1. Block diagram of the phone before and after the implementation of the module in the battery cavity of the phone.

To make room for TINA inside the phone the original battery is replaced by a smaller Casio NP-20 battery from a camera. This leaves $31 \times 34 \times 4$ mm^3 inside the phone that can house the module. Still the battery is capable of supplying both the phone and TINA for more than 1 hour of measurements.

The phone software does not allow us to use the phone's processors for logging the measured antenna parameters. Therefore TINA must include its own microprocessor system for data acquisition and interfacing.

The array of changes to the phone are shown in Fig. 1 where the standard phone is compared with the modified phone. Additional modifications include desoldering of the headset jack and using it for the USB link to the module, adding the hearing aid speaker very close to the main microphone and rerouting the antenna cables of the phone through TINA. Magnetic reed switches are used both for reset and on the battery supply of TINA. The reset switch closes in proximity of a magnet while the supply switch opens making it possible to power off TINA by placing the phone on a magnet. The addition of the power switch is necessary as TINA draws about 50 mA continuously resulting in severe battery drainage if left on overnight.

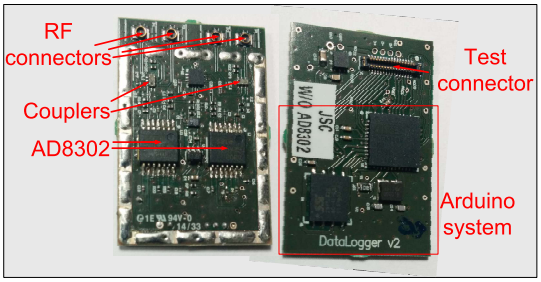

Fig. 2. Analog and digital side of TINA module. The analog side is normally covered by a shielding can which has been removed to reveal the RF circuitry.

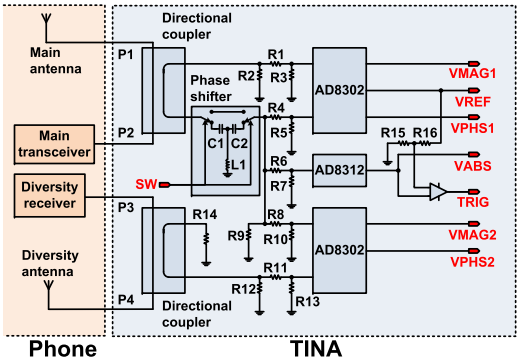

Fig. 3. Block diagram of the analog part of TINA and its interconnects with the phone. All ports are linking to the digital part.

A. TINA

The measurement system, TINA, consists of a $20 \times 30 \times 3$ mm^3 module that is built into the phone as shown in Fig. 1. The size of TINA is chosen as a trade-off between the space needed in the phone and the ease of designing the module itself. TINA can be separated into two parts: a) An RF part doing the network analysis and b) a digital microprocessor system controlling the RF part, storing the data and handling the measurement timing and user interface. Both sides of the module are depicted in Fig. 2.

The RF part of TINA is shown in Fig. 3. It is connected to the antenna lines of the phone such that the antenna signals go through the bidirectional couplers and a part of the power is coupled to the module while the rest is delivered to the antennas. To limit the sensitivity of TINA outside the bands of interest, band pass filtering could be applied to the coupled signals. This would increase the robustness to WIFI, Bluetooth and other RF signals from the phone itself. It was however chosen to omit such filters as the space required for such filters was not found. Instead, the WIFI and Bluetooth signals are turned off on the phone leaving only the GSM signal active. Three RF signals are acquired from the couplers; The transmitted signal from the GSM radio, the reflected signal from the main antenna and the received signal on the diversity antenna.

The core of the RF signal processing is formed by two AD8302 gain and phase detectors. They can measure the amplitude and phase difference between two RF signals, INPA and INPB. This is a very old chip that suffers from several imperfections. In particular, the amplitude output of the AD8302 is dependent on both phase and amplitude difference between the two RF inputs as seen in TPC 24 of [14]. For this reason a full calibration across the whole Smith Chart and for several frequencies is chosen instead of any faster technique relying on predicted behavior of the system. The AD8302 has an input range of each of its RF inputs of -60 to 0 dBm. It can measure differences in input power of the two inputs up to ± 30 dB. This sets the upper bound of the dynamic range to 60 dB. The dynamic range is limited further by the 33 dB power range of the GSM signal resulting in a dynamic range that decreases from close to 60 dB at maximum power to less than 30 dB at the lowest power level of GSM. This is acceptable for the current application as reflections lower than -6 dB and coupling between the antennas lower than -10 dB are acceptable and both reflections and coupling lower than -20 dB are so far from the limit that they effectively are not of interest. The top AD8302 in Fig. 3 is comparing the forward and the reverse signal on the main antenna line. This gives us the reflection coefficient from the main antenna. The bottom AD8302 compares the signal from the main transceiver to the received signal on the diversity antenna. This gives the coupling between the two antennas. The outputs of the AD8302 are two voltage signals where one, VPHS, is proportional to the difference in phase between the two RF input signals and the other, VMAG, is proportional to the quotient of the amplitude of the two RF input signals.

$$\text{VPHS} = \|\angle\text{INPA} - \angle\text{INPB}\|\,, \quad \text{VMAG} = \frac{V_{\text{INPA}}}{V_{\text{INPB}}} \qquad (1)$$

As Equation (1) shows, VPHS reports the absolute difference between INPA and INPB. Therefore $\angle$INPA $-$ $\angle$INPB will give the same voltage as $\angle$INPB $-$ $\angle$INPA. This is not acceptable for this purpose and therefore a phase shifter in the form of a high pass filter is added to the signal from the transceiver. This will phase shift the signal by approximately 90° at 900 MHz and 45° at 1800 MHz. By switching the signal to either bypass the filter or go through it, two different phase results are obtained and the combination of these results is unique. The real phase can thus be determined by doing these two measurements.

All the RF signals from the couplers are attenuated through resistive networks to achieve the desired RF powers of between -60 and 0 dBm for all power control levels (PCLs) of the GSM system and all mismatches. The component values of all discrete components on Fig. 3 are listed in Table I. The couplers are delivered under NDA and can thus not be described in detail. They are 0.8 by 1.6 mm and characterized from 699 to 2690 MHz with an insertion loss smaller than 0.23 dB typical and 0.36 dB worst case. The coupling factor changes from -27 dB in low bands to -20 dB in high bands.

TABLE I
VALUES OF DISCRETE COMPONENTS USED IN RESISTIVE NETWORKS, PHASE SHIFTER AND VOLTAGE DIVIDER FOR THE TRIGGER VOLTAGE LEVEL. 'NM' IS NOT MOUNTED.

R1	0 Ω	R2	NM	R3	56 Ω	R4	130 Ω
R5	30 Ω	R6	130 Ω	R7	1 kΩ	R8	130 Ω
R9	3.3 kΩ	R10	30 Ω	R11	0 Ω	R12	NM
R13	56 Ω	R14	50 Ω	R15	1 kΩ	R16	13 kΩ
C1	3.9 pF	C2	3.9 pF	L1	9.1 nH		

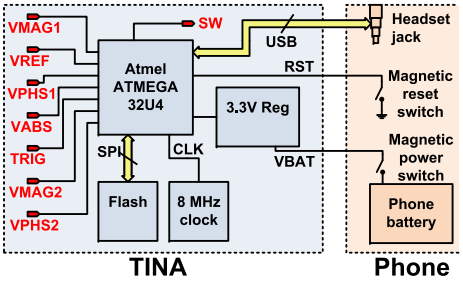

Fig. 4. Block diagram of the digital part of TINA and its interconnects with the phone. All ports are linking to the digital part.

The resistive networks at the top and bottom are currently configured for minimum attenuation. R2 and R12 are not mounted, R1 and R11 are 0 Ω (short circuits) and R3 and R13 are, together with the input impedance of the AD8302's, presenting 50 Ω impedance to the traces. The resistive network on the branch from the phase shifter is used to split the power of the main transceiver signal into three branches; One for the top AD8302, one for the bottom AD8302 and one for an absolute power detector, the AD8312 [14] in the middle which is used to gauge the PCL of the phone on VABS and, together with a comparator, to generate a burst trigger signal, TRIG. The comparator gets a reference signal from the top AD8302 which is divided resistively to 200 mV, so when the output of the AD8312 exceeds 200 mV the trigger signal goes high. This corresponds to an output signal of about -5 dBm out of the main transceiver.

The five analog voltages from the three detectors are fed to the digital part of TINA along with the burst trigger and the reference voltage from the top AD8302. The digital part of TINA is depicted in Fig. 4. An Arduino [**?**] minimum system is implemented on TINA to control the measurements. By choosing the Arduino platform the programming is made substantially easier and many prebuilt functions can be used. The digital part controls the phase shifter in the RF part, reads the voltages with its ADC inputs and saves the data. The communication with TINA is handled via USB. To completely hide TINA inside the phone the USB connection is attached to the phones headset connector.

An interrupt routine is implemented to read the ADCs synchronized to the burst by using the TRIG signal from the RF part. This is the basis of the user test. When TINA is put into trigger mode it also generates a sequence of tones to the

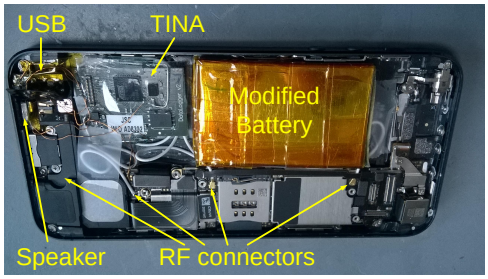

Fig. 5. Inside of the modified iPhone 5. Smaller battery, redirected antenna cables, USB connection through headset jack and a hearing aid speaker close to the microphone.

hearing aid speaker to keep the GSM link active at all times. The level of the hearing aid speaker is adjusted such that it can be heard at the other end of a call but not by the user of the DUT.

On top of the Arduino minimum system the digital part contains an 8 MHz clock circuit, a voltage regulator to supply the module with 3.3 V and a memory chip for saving the data. The power for the module is obtained from the phones battery.

B. Test procedure

Based on the blocks described above, the measurement system is run and data about the phone are acquired. There are three main tasks to perform to retrieve the reflection and coupling parameters of the phone antennas: calibration, measurement and post processing. Their individual flow charts are depicted in Fig. 6 while a more detailed description is given in this section.

First task is to calibrate the module. TINA contains a large analog part that has certain tolerances. These tolerances affect the accuracy of the system and must therefore be calibrated. By calibrating the module in many impedance points across all phases, the inaccuracies of the components are taken into account. Both the AD8302's, the phase shifter, the resistive attenuator networks and the couplers add uncertainties, many of which are mismatch dependent. Therefore it is concluded that the full range of impedances must be calibrated. As the frequency of operation is also important, TINA is calibrated at both high, middle and low channel in both the EGSM and the DCS band. The calibration is done using the calibration setup shown in Figure 7. It consists of a computer running LabView, a signal generator, a circulator and an impedance tuner. Fig. 8 shows the two different setups that are made from these components; A) and C) for reflection (S11) calibration and B) and D) for coupling (S21) calibration. The list of equipment is included in Table II.

The tuner itself needs to be calibrated with the setup shown in Fig. 8 A). For this calibration, the standard Maury software is used to make an adaptive calibration. The number of calibration points is adaptively determined by the software and lies between 250 and 300 points depending on frequency. One issue with the tuner is that the maximum voltage standing wave ratio (VSWR) is lower than desired. With a maximum

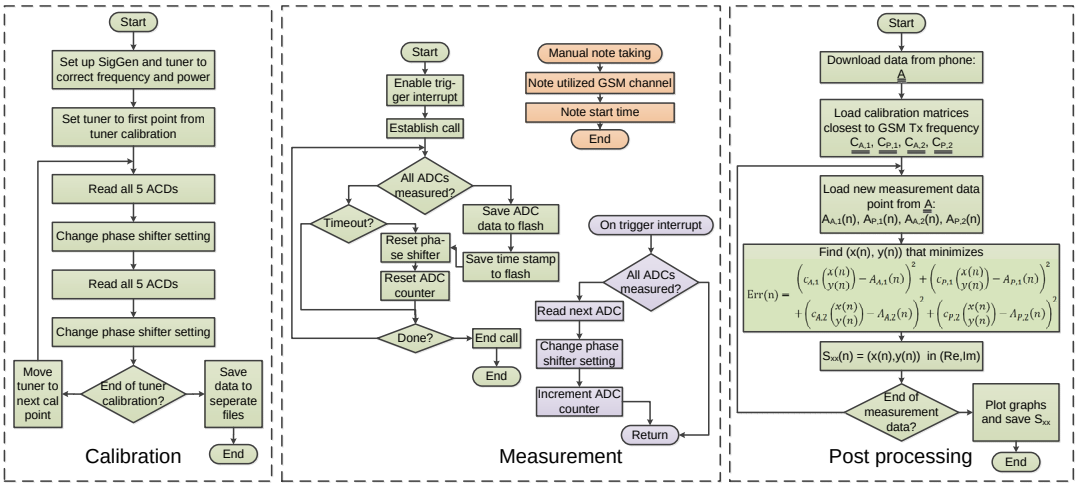

Fig. 6. Flow charts of the three main procedures in the system; The calibration of the module, the measurement inside the phone and the post processing of the results from the measurements.

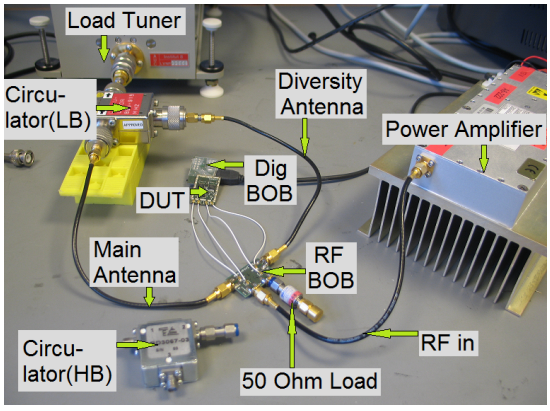

Fig. 7. Picture of the calibration setup. RF BOB and Dig BOB are break-out boards designed to make easy connections to TINA during calibration.

TABLE II
EQUIPMENT USED FOR THE CALIBRATION OF THE MODULE

Instrument	Model
R&S Signal generator	SME 06 [15]
R&S Vector network analyzer	ZVB 8 [16]
Maury Impedance tuner	MT982B01 [17]
Circulator for 890 - 915 MHz	Celwave BC900
Circulator for 1805 - 1880 MHz	Temex BD3067-03

of 9:1 in EGSM and 7.5:1 in DCS the calibration can only cover return losses down to 1.9 dB in EGSM and 2.3 dB in DCS. It would have been desirable to be able to measure greater mismatches but this cannot be done with the current calibration method. Once the tuner is calibrated, the primary

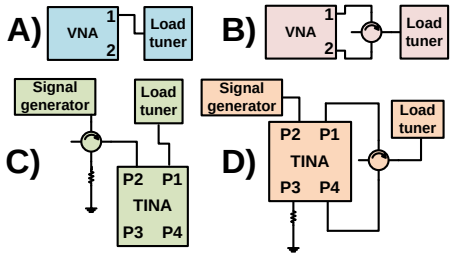

Fig. 8. Setup diagram for the module calibration. A) is for tuner calibration for the reflection branch and B) for the coupling branch of the module. C) and D) show the respective module calibration setups used for reflection and coupling.

branch of TINA is inserted as shown in Fig. 8 C) and the tuner is swept to exactly the same points as are used for the tuner calibration and the ADC's of TINA are read back. A calibration file is saved where the ADC values from TINA are linked to the reflection coefficient of the tuner. This file is later used for translation of the ADC points measured under test to S_{11}.

For the coupling branch of the module a slightly different calibration setup is required. Here the tuner is used to generate a reflected signal with a known phase and amplitude compared to the incoming signal. By feeding the signal into the tuner through the circulator, the reflected signal can be separated from the incoming signal and measured by Port 2 of the VNA as shown in Fig. 8 B). The tuner and circulator are then connected between the primary antenna port, P1, and the secondary antenna port, P4, of TINA as shown in Fig. 8 D). As for the reflection coefficient, the tuner is again swept through

all its' calibrated points and a file is saved that links the S_{21} measured in Fig. 8 B) to the ADC values of TINA for the corresponding tuner settings in Fig. 8 D).

The module only measures and stores ADC values. It is thus not needed to upload the calibration files to the module. Instead the calibration files are saved on a server for use during the post processing. A Matlab script is used to make an oversampled map of ADC values all across the Smith chart. A uniformly spaced matrix of 200 by 200 points is made by interpolating the measured ADC values.

To perform measurements the triggered mode is enabled through a serial command and thereafter the phone will record ADC values every time a burst is detected. The measurement time of TINA is very short. It is found to be possible to reliably measure three ADC values in each burst. It is thus chosen to measure both VMAG and VPHS from one AD8302 and VABS in the same burst. In the first burst VMAG1 and VPHS1 are measured with phase shifter setting 1 (SW1). In the next burst the same AD8302 is read with setting 2 of the phase shifter (SW2). In the two next bursts the same measurements are made for VMAG2 and VPHS2. The total measurement sweep of TINA takes 4 bursts or 18.46 ms. A sample rate of more than 50 Hz is therefore possible. 10 Hz is deemed enough to catch even fast changes and to limit the memory usage this is the chosen sampling rate.

The timing of the bursts is recorded by adding a time stamp for each complete ADC sweep. The time stamps run off an internal clock and are thus not very precise but only an approximate timing information is needed. The only use of the time stamps is finding the approximate time of an event to find the cause of the event on video recordings of the measurement. To convert the internal clock to that of the computer a time stamp is recorded when the triggered mode is enabled and for each full sweep of ADC values. By comparing the time between these time stamps to the difference in value, the time step of the module clock can be found.

After a user measurement is done the data are downloaded to the computer and the post processing tools are used to convert the raw ADC values from the measurement to reflection and transmission coefficients. The post processing tool uses the calibration files to do the conversion according to the formula shown in the biggest green box of Fig. 6. The function determines, for every time step in the measured data, the squared difference between the measured ADC value and each point in the corresponding calibration matrix. It then adds these difference matrices for each phase shifter setting and both amplitude and phase measurements to get an overall difference matrix. By finding the minimum of this matrix, the least square residual is found and this point is believed to be the closest to point in the matrix to the measured ADC values. Since the matrix is a 200 by 200 value matrix uniformly spaced across the Smith Chart, the index of the least square residual can be converted to a complex S-parameter value simply by counting the distance in indices from the center of the Smith Chart and divide it by 100. The calibration files map the ADC values of the different ADC's across the Smith chart. Ideally VMAG should be constant for constant VSWR and VPHS should change linearly with phase. As earlier mentioned, this

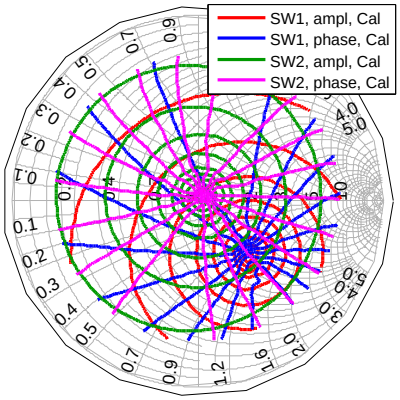

Fig. 9. Contour plot of the calibration data in the impedance Smith Chart with $Z_L = 50\Omega$. SW1 is with phase shifter in setting 1 and SW2 is with phase shifter in setting 2.

is not the case for the AD8302 as can be seen on Fig. 9. Clearly the calibration done with switch setting 2 gives the most optimum performance where the maximum value is close to the center of the Smith chart. The offset with switch setting 1 is larger because the high pass filter of the phase shifter is close to its cutoff frequency. This results in an impedance far from 50 Ω, which impairs the performance of TINA all together. For a future design, a delay line could be used for phase shifting to avoid this effect.

Fig. 10 shows an example of the output of the post processing algorithm. An ADC sweep is chosen from the output file of the phone. The values were VPHS_{SW1} = 232, VMAG_{SW1} = 518, VPHS_{SW2} = 343 and VMAG_{SW2} = 514. The calibration contours equal to these values are highlighted in Fig. 10. As can be seen the VMAG_{SW2} contour crosses the VPHS_{SW2} contour in two places. The VPHS_{SW1} contour coincides with the two other only in the upper crossing point. This is a clear indicator that this is the point of interest. The shown example is for the reflection coefficient but exactly the same procedure is used for the coupling coefficient.

When all ADC sweeps in the measurement series have been converted to reflection and coupling coefficients, a full series of coefficients versus time is obtained. This can be analyzed to find the range and rate of change of the coefficients. The following part contains the full set of data and analyses that were obtained from the initial measurement campaign.

III. RESULTS

This section contains the results that are obtained from the test setup described in the previous section. The results are split into two parts: a calibration accuracy study and a set of preliminary user data collected using TINA inside the iPhone.

A. Calibration accuracy

It is chosen to calibrate at low, mid and high channel for the GSM900 and the GSM1800 bands as these are the bands that are in use for the 2G networks in Denmark. The module

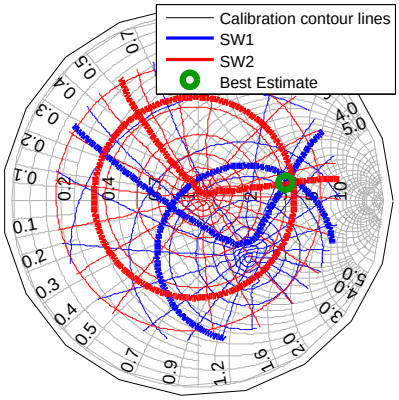

Fig. 10. Estimation of the reflection coefficient based on calibration data and a set of measured data points from the phone plotted in an impedance Smith Chart normalized to 50 Ω. The highlighted contours are the calibration contours matching the measured data points.

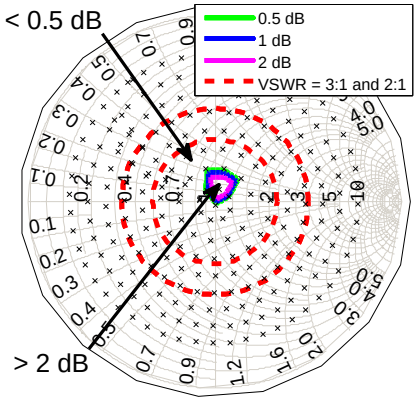

Fig. 11. The difference in amplitude calibration between 0 dBm and 30 dBm S_{11} calibration power for DCS band on TINA1 plotted in an impedance Smith Chart with $Z_L = 50\Omega$. The 0.5, 1 and 2 dB contour lines are shown as well as the constant VSWR circles for 2:1 and 3:1. The error is less than 0.5 dB for the majority of the calibration points with a very sharp spike in error close to the center of the Smith Chart. The black markers are showing the actual calibration points.

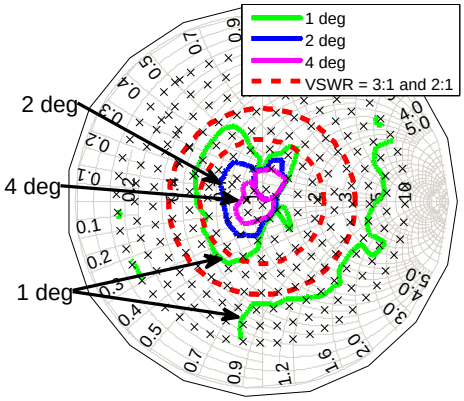

Fig. 12. The difference in phase calibration between 0 dBm and 30 dBm S_{11} calibration power for DCS band on TINA1 plotted in an impedance Smith Chart with $Z_L = 50\Omega$. The 1, 2 and 4 degrees contour lines are shown as well as the constant VSWR circles for 2:1 and 3:1. The black markers are showing the actual calibration points.

is designed to support all power levels of the 2G standard (5 to 33 dBm in GSM900 and 0 to 30 dBm in GSM1800). To ensure accurate results, the first modules, TINA1 and TINA2, are calibrated at 0, 10, 20 and 30 dBm for high band and 5, 14, 24 and 33 dBm for low band.

To verify that the calibration is repeatable and to investigate the reference power dependence of the calibration, a comparison is made between the calibration values for the highest and the lowest reference power level. Figures 11 and 12 show an example of a comparison. Here, TINA calibration at 1747 MHz and for switch setting 2 is chosen. The contour lines for selected differences are plotted along with the constant VSWR circles for 3:1 and 2:1. These two VSWR circles are plotted because they represent the -6 dB and -10 dB reflection/coupling level which are the most important levels when testing the phone. Finally, to illustrate the quantity and position of the calibration points, the complete calibration point constellation is plotted on top as black markers. It can be seen on these figures that the main uncertainty is concentrated where the reflected/coupled power is low. For the power, this is well inside the smallest VSWR circle meaning that the S-parameters are far below -10 dB. The uncertainty on phase is more spread out when looking at the range from 1 to 4 degrees.

The cumulative distribution function (CDF) of the difference in calibration values between highest and lowest power level can be seen in Figures 13 and 14 for amplitude and phase calibration, respectively. Only the minimum and maximum powers (0 and 30 dBm for DCS and 5 and 33 dBm for EGSM) are used since this gives the worst case error which is especially centered around the middle of the Smith Chart where the reflected and coupled signals get below the sensitivity of the AD8302. Here the calibration difference between the maximum and minimum power level can reach the full power difference between lowest and highest power, when the reflection or coupling reaches the noise floor. Any power level in between will give less error. Each CDF is made based on all calibration points at all frequencies of the band with both switch settings and for both S_{11} and S_{21}. These plots do thus, collectively on all four non-temperature dependent graphs, incorporate the complete comparison between highest and lowest power level for all conditions on both modules.

TINA2 has also been calibrated in high band (HB) at 10°C and 55°C as well. The CDF of the variation over temperature can be seen in Figures 13 and 14 too.

B. User test results

As an overall system test a short measurement series is made with the modified phone for a small series of use

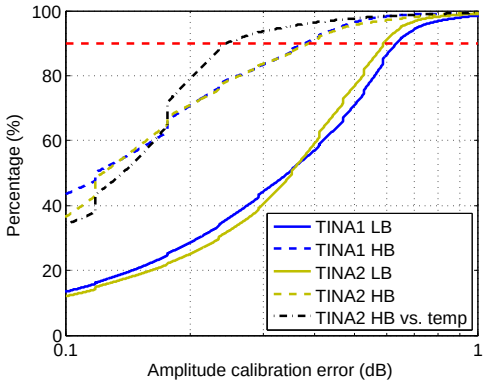

Fig. 13. Cumulative density function (CDF) of the variation for amplitude calibration for high and low band on two different modules. The black curve is showing variation over temperature between 10°C and 55°C.

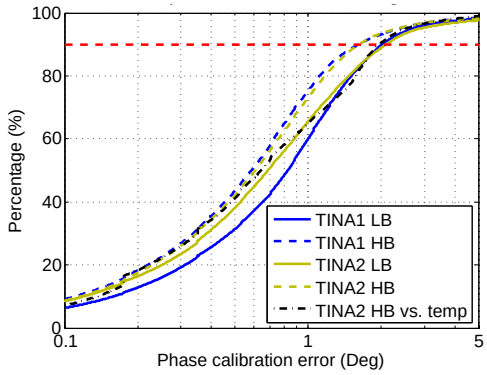

Fig. 14. Cumulative density function (CDF) of the variation for phase calibration for high and low band on two different modules. The black curve is showing variation over temperature between 10°C and 55°C.

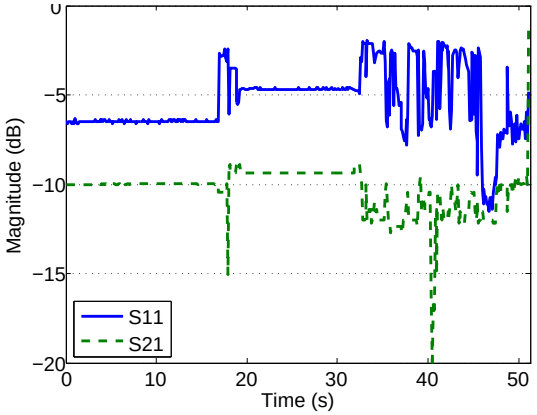

Fig. 15. Magnitude of the mismatch of the main antenna and coupling between the antennas versus time measured on the iPhone5 with TINA during test with a user.

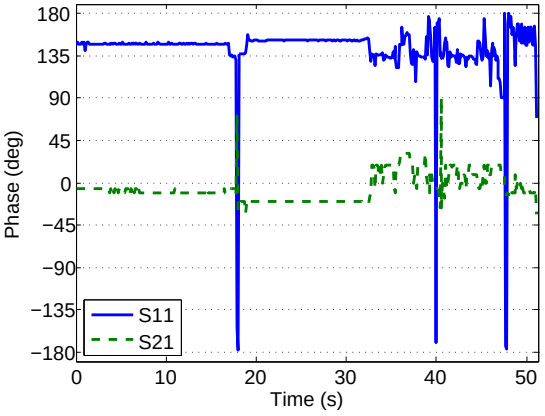

Fig. 16. Phase of the mismatch of the main antenna and coupling between the antennas versus time measured on the iPhone5 with TINA during test with a user.

cases. A time series of the magnitude of the reflection and coupling is plotted in Fig. 15. Fig. 16 shows the phase of the reflection and coupling between the phone's antennas for the same measurement. The measurement consists of a period where the phone is left on a Styrofoam block to measure the S-parameters in free space. Afterwards the phone is placed on a copper plate to measure it in a harsh but static environment. Finally the phone is handled by a test person who tries to change grips as much as possible to achieve a very dynamic user scenario.

IV. DISCUSSION

From the calibration data obtained for this study it is seen that the calibration accuracy is quite good. The calibration values change mostly close to the center of the Smith Chart. The region with significant changes is well within the 2:1 constant VSWR circle and thus only when the match is very good will these inaccuracies be seen. A difference of a dB does not matter in this region where the reflection is already down to -20 dB. As for the phase difference, it is more spread out in the Smith Chart. Since the main focus of this study is on accurately determining the magnitude of the reflection and coupling it is chosen to accept the error in phase.

90% of the values are within 0.6 dB for the amplitude and 2° for the phase. This is the worst case error due to difference in transmit power if the same calibration data are used for all power levels. It can be minimized by reading the on-board power meter for each burst and applying the calibration values obtained at the closest PCL. However, an error of this magnitude is considered acceptable and shows that the attenuation of the signals in the RF part of TINA is well adjusted to the power range in GSM. As can be seen in Figures 13 and 14 there is a comparable difference across temperatures from 10°C to 55°C. This is accepted as an added

uncertainty and thus the temperature inside the phone is not measured.

The highest inaccuracies are recorded close to the center of the Smith chart where the reflection and coupling are low. In this area of the Smith chart very small absolute changes lead to large changes in dB. It is thus expected that the inaccuracy in dB is high for this region.

As can be seen from Figures 15 and 16, the effect of the surrounding environment is clearly seen on the measured S-parameters. When the phone is left on the Styrofoam block, the magnitudes of the mismatch and coupling are very stable at -6.5 dB and -10 dB, respectively. These levels are in line with the normal design goal of mobile phone antennas of lower than -6 dB reflection. The phase of the S-parameters is quite stable which is to be expected since the phone is in a very stable position with no physical interaction. The influence of frequency hopping is not seen. This is because the frequency spread of the hopping sequence is only a few MHz which translate into negligible phase shifts for the RF line length of TINA.

When the phone is moved onto the copper plate, the mismatch changes to -4.7 dB. The coupling changes to -9.3 dB. It is to be expected that the reflection will be more dominant on the highly conductive surface. Still the coupling between the antennas is slightly increased and taking into account the reflection this means that a much larger portion of the emitted signal of the main antenna is absorbed by the diversity antenna. For this scenarios the phase is very stable as well.

For the final scenario, where the user is handling the phone and changing the grip rapidly, it is seen that the S-parameters of the antennas are also very fluctuating. The performance is generally poor with reflections often reaching -3 dB and worse. This is in line with previous studies on the iPhone5 that show extensive performance degradation in the presence of the user [18]. At the end of the measurement, a section with low reflection is recorded. In this section, the lossy tissue of the user is believed to absorb so much power that the match of the antenna is improved.

V. Conclusion

This study shows an original approach to S-parameter measurements on electrically small antennas. A system has been designed and implemented that can measure reflection and coupling for a two-antenna system. It is proposed for any small wireless system such as wireless sensors, mobile phones and wireless Internet devices.

To demonstrate the principle of the system, it is built into a fully functional commercially available phone. The system can measure the S-parameters of the phone antennas while the phone is in a call. The system consists of a main board, TINA, containing RF circuitry to measure amplitude and phase of both the reflection on the main antenna and the coupling to the diversity antenna. This is very hard to measure with a normal VNA because of the cable effect and even more challenging on a production phone with a user interacting with the phone.

The initial calibration data collected for TINA show good stability over temperature and phone output power. With an accuracy of approximately 0.6 dB and 2° for 90% of the measurement points, TINA can easily estimate any mismatch and coupling coefficient accurately enough for designing an active antenna tuner.

Even though the measurement system must be designed specifically for the DUT it is still seen as the best way to achieve accurate user test results. Any other method known to the authors either include cables or optical fibers obstructing the user. If one could fit a fully coherent transceiver inside the DUT it should in principle be possible to extract the phase and amplitude of the reflection by adding a coupler and using the receiver to demodulate the reflected wave from the antenna. Such capabilities could exist in the GSM transceiver of some modern smart phones but they are not available to the research community.

The introduction of this new measurement system enables tests that would otherwise be impossible to make. It will be possible to investigate the dynamics of the user effect without having obstructing cables hanging out of the phone. This enables true blind testing of the phones eliminating the risk that users may handle the phone differently because they know that the antennas are being tested.

Acknowledgment

This work is part of the Smart Antenna Front End (SAFE) project funded by Innovation Fund Denmark.

References

[1] H. Wheeler, "Small antennas," *IEEE Transactions on Antennas and Propagation*, vol. 23, no. 4, pp. 462–469, Jul 1975.

[2] M. Salehi and M. Manteghi, "Transient characteristics of small antennas," *IEEE Transactions on Antennas and Propagation*, vol. 62, no. 5, pp. 2418–2429, May 2014.

[3] W. Kotterman, G. Pedersen, K. Olesen, and P. Eggers, "Cable-less measurement set-up for wireless handheld terminals," in *12th IEEE International Symposium on Personal, Indoor and Mobile Radio Communications*, vol. 1, Sep 2001, pp. B–112–B–116 vol.1.

[4] T. H. Loh, M. Alexander, P. Miller, and A. Lopez Betancort, "Interference minimisation of antenna-to-range interface for pattern testing of electrically small antennas," in *Proceedings of the Fourth European Conference on Antennas and Propagation (EuCAP)*, April 2010, pp. 1–5.

[5] D. Ji, J. Jeon, and J. Kim, "A novel load mismatch detection and correction technique for 3g/4g load insensitive power amplifier application," *IEEE Transactions on Microwave Theory and Techniques*, vol. 63, no. 5, pp. 1530–1543, May 2015.

[6] S. Sussman-Fort and R. Rudish, "Non-foster impedance matching of electrically-small antennas," *IEEE Transactions on Antennas and Propagation*, vol. 57, no. 8, pp. 2230–2241, Aug 2009.

[7] P. Sjoblom and H. Sjoland, "Constant mismatch loss boundary circles and their application to optimum state distribution in adaptive matching networks," *IEEE Transactions on Circuits and Systems II: Express Briefs*, vol. 61, no. 12, pp. 922–926, Dec 2014.

[8] A. van Bezooijen, M. de Jongh, C. Chanlo, L. Ruijs, F. van Straten, R. Mahmoudi, and A. van Roermund, "A gsm/edge/wcdma adaptive series-lc matching network using rf-mems switches," *IEEE Journal of Solid-State Circuits*, vol. 43, no. 10, pp. 2259–2268, Oct 2008.

[9] R. Lao, W. Liang, Y.-S. Chen, and J. Tarng, "The use of electro-optical link to reduce the influence of RF cables in antenna measurement," in *IEEE International Symposium on Microwave, Antenna, Propagation and EMC Technologies for Wireless Communications*, vol. 1, Aug 2005, pp. 427–430 Vol. 1.

[10] B. Yanakiev, J. Nielsen, M. Christensen, and G. Pedersen, "Long-range channel measurements on small terminal antennas using optics," *IEEE Transactions on Instrumentation and Measurement*, vol. 61, no. 10, pp. 2749–2758, Oct 2012.

[11] S. Saario, D. Thiel, J. Lu, and S. O'Keefe, "An assessment of cable radiation effects on mobile communications antenna measurements," in *IEEE Antennas and Propagation Society International Symposium*, vol. 1, July 1997, pp. 550–553 vol.1.
[12] Gerfried Palme, *Measurements with the DG8SAQ VNWA 2/3 Vector Network Analyzer*, October 2015.
[13] A. Tatomirescu and G. Pedersen, "Body-loss for popular thin smart phones," in *7th European Conference on Antennas and Propagation (EuCAP)*, April 2013, pp. 3754–3757.
[14] *AD8302, LF2.7 GHz RF/IF Gain and Phase Detector*, Analog Devices, Inc., 2002, Data Sheet: Rev. A.
[15] *Rohde and Schwarz SME06 Operating Manual*, Rohde and Schwarz GmbH, 1999, Data Sheet: 1039.1856.12-14-.
[16] *Rohde and Schwarz ZVB Network Analyzer*, Rohde and Schwarz GmbH, 2011, Data Sheet: v08.02.
[17] *MT982 SERIES SENSOR TUNERS*, Maury Microwave Inc, 2012, Data Sheet: 4T-078.
[18] A. Tatomirescu and G. Pedersen, "User body loss study for popular smartphones," in *9th European Conference on Antennas and Propagation (EuCAP)*, 2015.

Emil F. Buskgaard received the M.Sc. E. E. degree from Aalborg University, Denmark in 2005. Currently he is a PhD student in the Antenna, Propagation and Networking group at Aalborg University. He's primary interests are related to research, design and automation of RF test systems and the user intaraction with electrically small antennas for mobile devices. Prior to his research role, he has worked for 7 years with RF design and verification at SiTel Semiconductor B.V. and Broadcom Inc. He holds 2 granted and pending patents.

Ben K. Krøyer received his Electro Technicians Diploma from Odense Technicum, Denmark, in 1998. He has been employed at Aalborg University, Institute of Electronic Systems, since 1999, taking care of a variety of hardware tasks within the components workshop until 2001. Hereafter he has been responsible for hardware and firmware design as well as antenna prototyping and PCB fabrication. His interests are general hardware and software development of prototype platforms.

Alexandru Tatomirescu , born in January 1987, has received a bachelors degree in Electronics and Telecommunication from the Polytechnic University Bucharest (2009), a Master degree in Mobile Communications from Aalborg University (2011) and a PhD degree (2014) in Antenna design from the same university . Currently, he is working as an assistant professor at Aalborg University on mobile antenna design and nanosatellite antennas. His main topics of research include mobile phone antenna design, reconfigurable antennas, antenna decoupling, satellite antennas, beam-steered antennas and the practical limits of electrically small antennas. He is an active IEEE member and he is participating in the COST IC1004 action.

Ondřej Franek (S'02–M'05) was born in 1977. He received the M.Sc. (Ing., with honors) and Ph.D. degrees in electronics and communication from Brno University of Technology, Czech Republic, in 2001 and 2006, respectively. Currently, he is working at the Department of Electronic Systems, Aalborg University, Denmark, as a postdoctoral research associate. His research interests include computational electromagnetics with focus on fast and efficient numerical methods, especially the finite-difference time-domain method. He is also involved in research on biological effects of non-ionizing electromagnetic radiation, indoor radiowave propagation, and electromagnetic compatibility.

Dr. Franek was the recipient of the Seventh Annual SIEMENS Award for outstanding scientific publication.

Gert Frølund Pedersen was born in 1965 and married to Henriette and have 7 children. He received the B.Sc. E. E. degree, with honour, in electrical engineering from College of Technology in Dublin, Ireland, and the M.Sc. E. E. degree and Ph. D. from Aalborg University in 1993 and 2003. He has been employed by Aalborg University since 1993 where he is now full Professor heading the Antenna, Propagation and Networking group and is also the head of the doctoral school on wireless which some 100 phd students enrolled. His research has focused on radio communication for mobile terminals especially small Antennas, Diversity systems, Propagation and Biological effects and he has published more than 75 peer reviewed papers and holds 20 patents. He has also worked as consultant for developments of more than 100 antennas for mobile terminals including the first internal antenna for mobile phones in 1994 with lowest SAR, first internal triple-band antenna in 1998 with low SAR and high TRP and TIS, and lately various multi antenna systems rated as the most efficient on the market. He has been one of the pioneers in establishing over-the-air measurement systems. The measurement technique is now well established for mobile terminals with single antennas and he was chairing the COST2100 SWG2.2 group with liaison to 3GPP for over-the-air test of MIMO terminals.

Paper E

Large-scale Experimental Study of the User Effect on Live Mobile Phones

Emil Feldborg Buskgaard, Ben K. Krøyer, Ondrej Franek, Gert Frølund Pedersen

The paper has been drafted for the
IEEE Transactions on Antenna and Propagation, 2016.

Large-scale Experimental Study of the User Effect on Live Mobile Phones

Emil Buskgaard*, Ben Krøyer*, Ondrej Franek*, Gert Frølund Pedersen*
*Section of Antennas, Propagation and Radio Networking (APNet), Department of Electronic Systems,
Faculty of Engineering and Science, Aalborg University, DK-9220, Aalborg, Denmark
{eb, bk, of, gfp}@es.aau.dk

***Abstract*—As hand-held antenna systems are becoming more and more dynamic they acquire the ability to compensate for the adverse effects of the user. Such antenna systems cannot be tested sufficiently in a static measurement setup as this will not test the ability of the antenna tuning to correctly compensate for the user as he/she changes grip on the phone. Therefore, a novel measurement system is developed where a complete network analyzer is built into the phone enabling measurements without any cables or fibers coming out of the device. Such a system is allowing the user to interact normally with the phone and thereby realistic data can be collected on the range and rate of change in the S-parameters of the phone. A large-scale measurement campaign on 100 users has been performed giving the first ever statistical S-parameter data from a fully functional phone, an iPhone 5s, in a live network. The data show that the phone under test has very low coupling between the Main antenna and the diversity antenna while the reflection coefficient of the main antenna is poor for low bands and low power levels. The rate of change of S_{11} found to be very fast for certain types of events resulting in S_{11} changing from -6 dB to -2 dB in just 0.2 s. This is valuable input to anybody designing closed loop antenna tuning. The technology behind the TINA is still new and the data are not yet of comparable quality to those of a box instrument. This is still a very promising first step on the way to true network analysis inside a mobile phone.**

***Index Terms*—Measurement techniques, Mobile antennas, 4G mobile communication, Antenna measurements, MIMO**

I. INTRODUCTION

PERFORMANCE of mobile phone antennas has been the subject of much discussion recently. Recent studies show that phone antennas in current smartphones are performing poorly both in free space and in the presence of the user [1]. The reason for this may be the high demand for multi-band coverage and small size. Additionally the requirement for multiple-input multiple-output (MIMO) and diversity means that several antennas are needed and that they have to be adequately decorrelated even though they both reside in the same limited space.

As the reliability and performance of antenna tuners improves, tunable antennas are looking more and more like the best candidate to improve antenna performance and enable further miniaturization of mobile phone antennas [2], [3]. There are many practical issues to overcome. Several are caused by the dynamic nature of such a system. It is no longer enough to make static measurements on the antenna as it may have good performance in free space or with one specific grip but face much degradation due to the user touching the phone in other positions. As the antenna can be re-tuned, the detuning effect of the user can be canceled [4], [5]. This sets increased requirements to the antenna tuning circuit as it must be able to follow the dynamic changes in the reflection coefficient as the environment around the phone changes.

Before such systems can be designed, an understanding of the dynamics of the user effect must be obtained. It is important to know the range of reflection coefficients seen by the system as well as the rate of change in the reflection coefficient meaning how fast the coefficients can change. Current measurement techniques are not fit for dynamic user effect measurements on tunable antennas. The classical way to measure antenna performance is far field measurements in an anechoic room [6], [7]. Such a measurement requires the antenna pattern and user interaction to be static for the duration of the angular sweep. This is not suitable for tunable antennas and certainly not sufficient to study the dynamics of the user influence on the antenna. Another common approach is to measure the antenna impedance as an S-parameter using a vector network analyzer (VNA). This measurement only evaluates the power transfer to the antenna and not the radiation efficiency. This is however the parameter that can be optimized by antenna tuning, so it is a good parameter to start with.

Several issues are seen in current S-parameter setups though. They all rely on a VNA attached to the phone by cables or optical fibers [8], [9]. Cabled measurements are the easiest but also the least accurate as the cable will perturb the electromagnetic fields close to the phone [10]. By using an optical link this is prevented but also this approach has drawbacks. The authors are not aware of any commercial optical two-way link that is capable of measuring S-parameters and the implementations found are all big compared to the size of a smartphone. This means that a large box will be attached to the phone and thus the user cannot grip the phone in a natural way. Furthermore the optical cables limit the freedom of movement of the user since they are either rigid or fragile or even both.

This study is based on a new class of antenna measurement devices, the tiny integrated network analyzer (TINA), that was first introduced in [11]. The benefit of the TINA is that it is small enough to reside inside the device under test (DUT). This eliminates the cabling both eliminating the cable effect and enabling the user to grip the phone in a natural and unrestricted way.

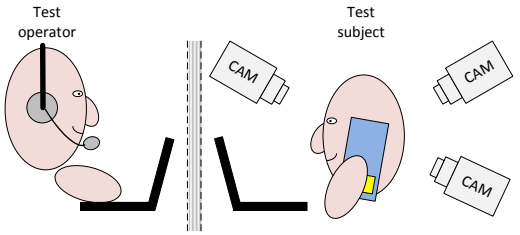

Fig. 1. Sketch of the test setup. A test subject sits in a room with camera surveillance, a spectrum analyzer, a PC and the test phone with the TINA inside (right). In another room (left) the test operator is talking to the test subject via the phone and instructing the test subject.

The test is performed in a setting as depicted in Figure 1. The study is made as a blind study in the sense that the test subjects are not aware that the antenna performance of the phone is being measured. The phone, an iPhone 5s, is made such that all changes are hidden completely inside the phone. We believe that this is the most realistic scenario to study the dynamic influence of the user on the phones antennas. It is a challenging approach as well. The measurement setup needs to be fully embedded in the phone and so well integrated on the antenna feed networks that the radiation performance of the phone is affected as little as possible.

This article describes this user study and the first experimental results on reflection and transmission ever published on a fully functional mobile phone on a live network. In Section II the concept and implementation of the measurement setup is described, Section III shows the statistical results of the measurement campaign and selected events in more detail. Section IV discusses the findings of the user study. Finally Section V concludes on the study and presents the next steps.

II. METHODOLOGY

This section describes the measurement setup as well as the test procedure of the user study. At the end of the section the measurement post processing is explained. For the user study an iPhone 5s is chosen since it was already explained in [11] how to prepare this phone for the test. Additionally, the iPhone 5s was a hugely successful phone at the time when this study started making it a logical phone to start with.

Two phones were prepared: one was used in the test, and the other by the test operator for data download, charging and restarting. In this way there was always a fully charged phone ready for the next test subject. Additionally, having two phones enabled the campaign to continue even if a phone broke down and gave the authors a way identify issues by comparing results between the phones.

A key goal for this study is to achieve the most realistic data possible for the user interaction with the phone. Since the TINA is very small it can be completely hidden inside the phone. The phone is still fully functional meaning that the user can use all of its functionalities without ever realizing that there is a measurement device inside. The user study was performed with the phones attached to a live network. The

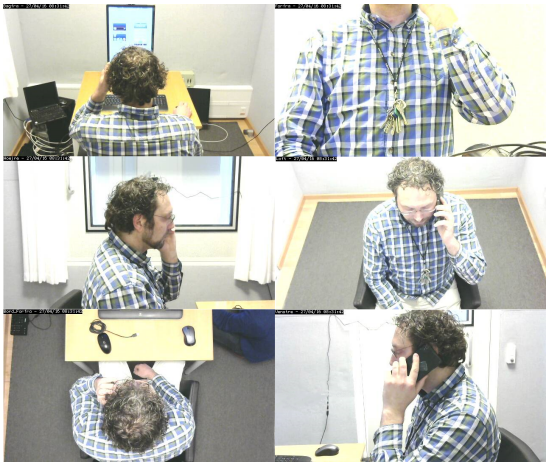

Fig. 2. Example footage from the 6 web cams of the experiment. The positions are chosen to give the most useful pictures of the test subject in both talk mode and data mode.

phones were set to 2G only to limit the output power range to approximately 30 dB and to ensure bursted transmissions that the TINA needs for triggering and synchronization. To blind the study the test subjects are told that they are participating in a usability study on a phone during a call. They therefore have to perform all tasks in call mode meaning that the transmit bursts are present for the TINA to function. The following section describes the measurement setup for the user study in more detail.

A. Measurement setup

The overall drawing of the measurement setup was shown in Figure 1. The measurement is made in a listening room where the test subject is placed in a chair in the middle of the room. In front of the test subject there is a table with a computer and around the room, 6 web cams are placed. The web cams are monitoring the experiment at a frame rate of 10 fps equal to the update rate of the TINA. This footage can later be used to visually inspect the occurrences if abnormal behavior is detected from the S-parameters. Figure 2 shows the web cam streams from the test facility where the test was performed. As can be seen the test subject is observed from front low, front high, back, right, left and above. This is done to give the best possible coverage of the test zone to increase the likelihood of capturing useful pictures of all events.

The computer is displaying a questionnaire that the test subject must fill in. The questionnaire instructs the test subject to perform and rate different tasks on the phone. This ensures that both call mode and one- and two-handed data mode is used during the course of the measurement. The test subject is not directly told how to grip the phone as this would lead to non-natural grips defeating the purpose of the blind study. In an adjacent room the test operator is situated. The test operator guides the test subject through the measurement. The test operator has a computer for enabling the TINA prior to

the measurement and downloading the data from the TINA after the measurement. The following section explains the test procedure in more detail.

B. Test procedure

An important part of the success of an experiment is a well prepared procedure for the test. Much effort has been put into making the test as easy and intuitive for the test subjects and the data collection as automated as possible for the test operators. A complete overview of the test procedure is given in Figure 3. Prior to any testing, the test facilities are set up as explained in the section above. The camera positions, brightnesses and contrasts are adjusted to give the best possible pictures of the test subject. Every morning, the setup is started up and checked and a free-space control measurement is performed on each phone and the results are saved for later analysis. Once the setup is verified the test subject is escorted to the room and after a short introduction to the questionnaire the test subject is left alone in the test room to complete the test.

The flow of the test itself can be seen in Figure 3D. The first step for the test subject is to call the test operator and talk to the test operator through the phone under test. Hereby, we obtain a period of data in talk mode. Thereafter, the test subject is asked to write an SMS message with the phone first in vertical position and thereafter in horizontal position. This urges the test subject to use both the one hand and the two hand data grips. Then the test subject is asked to go to a web page where the test subject must find a code on the top and bottom of the page. The page is constructed such that the test subject will have to scroll extensively meaning that a substantial amount of swiping will be recorded by the TINA. Finally, the user is asked to plug in the charging cable. The charging connector is situated in the middle of the antenna and plugging in the cable is expected to change the impedance radically and fast. Therefore, this event is interesting to include in the measurement.

To blind the study, the test subject is initially told that he/she is participating in a study to assess the usability of the phones' functions while in a call. This explains why the user cannot hang up the call which is important since the TINA relies on the transmitter for generating the RF signal for its VNA functionality. To support this the test subject must fill in a questionnaire during the experiment. In the questionnaire, the test subject must answer some questions after each part of the test. After each part of the questionnaire, a time stamp is saved in a log file. These time stamps can be used in post processing to do a first estimation of whether an event occurred in talk mode, or one of the different data modes. Also, the questionnaire includes data about age, gender and smartphone experience level that can be used to see if these parameters influence the test data.

After the test subject completes all tasks the call is terminated and the phone is handed back to the test operator. The test operator downloads the data from the TINA inside the phone and rearms the trigger before handing the phone to the next test subject. In the meanwhile the questionnaire answers are saved and the questionnaire is reset as well.

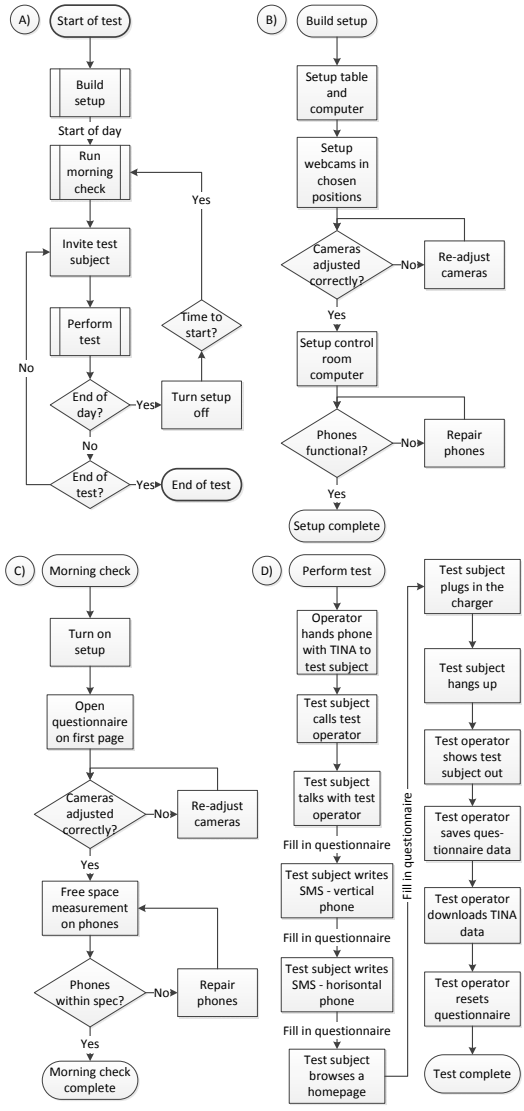

Fig. 3. Flow chart of A) the complete test procedure accompanied by flow charts for each subprocess: B) Construction of the setup, C) Daily start-up check procedure and D) the test itself.

After all data has been generated and saved to files, the post processing can commence as described in the next section.

C. Result post processing

The data from the measurements consist of ADC-values from the TINA, time information and answers from the questionnaire and video footage from the web cams. The video footage is stored as a series of jpeg pictures with time stamps

and requires no additional formatting. The questionnaire data are linked to the individual test subject at the time of saving and can thus be correlated with the ADC data afterwards. The ADC values from the TINA requires several steps of post processing before they can be used.

First, the ADC values are translated to S-parameter data as described in [11] by comparing them to previously obtained calibration values. For each measurement point, the ADC values for the reflection coefficient are compared to calibration data for 6 different frequencies and 4 different power levels. An error estimator is calculated based on the difference between the measured values and the closest matching point in the calibration. This error indicator is then compared for all frequencies and power levels and the combination with the lowest value is picked. The frequency and power is estimated accordingly. To increase the confidence in the data, the data points with high error indicator values are excluded from the final analysis.

For the coupling data a function was derived for the amplitude and phase. This enabled a finer resolution at the very low coupling levels that were generally observed. The same type of function was not found for reflection since the measured reflection data were generally valued and therefore in a region of the Smith Chart that could more accurately be measured directly and where the error of the derived function would be bigger than those of the raw calibration data.

The measurement data from the TINA are time stamped with the internal clock value of the micro-controller unit (MCU) clock for each measurement point. A time stamp is also saved when the TINA is activated (T_{start}) before the test and again when the data are read out of the TINA after the test (T_{stop}). These two time stamps are saved together with the corresponding calendar time stamps of the computer used to activate and save data from the TINA. The time stamps for the individual data point can thereafter be converted to calendar time by linearly interpolating between T_{start} and T_{stop}.

Based on these post processing steps, we have obtained a time series of S-parameter data with calendar time stamps and corresponding information about the test subject and video footage that shows the course of the experiment from six different angles. Based on these data, the following section will present the data and the statistical analysis of the data.

III. RESULTS

This section contains the results that are obtained from the test setup described in the previous sections. The results are split into two parts:a statistical analysis based on all of the obtained data and a qualitative analysis of selected events from the recorded data.

Based on all the acquired measurement data a statistical analysis is made. First analysis is shown in Figure 4 and shows a box plot of median, 25- and 75-percentiles, extrema and outliers of S_{11} when limited to different error values. As can be seen, the difference in especially 25- to 75-percentiles is visible between data limited at error values above 1000. This means that we choose to exclude data with more than 1000 in error value from the following data analysis.

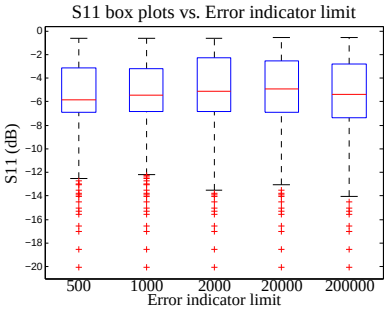

Fig. 4. Box plots for S_{11} for different error limits.

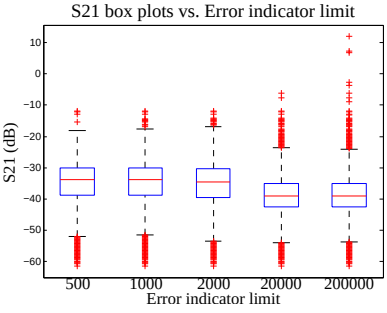

Fig. 5. Box plots for S_{21} for different error limits.

Figure 5 shows S_{21} between the two antennas for the same error limits. Here, data all the way to 2000 have very similar statistical distributions. For simplicity and to stay conservative, we choose to cut S_{21} data at an error value of 1000 as well.

With the error limit building confidence in the remaining data, we continue to explore which factors influence S_{11} and S_{21} the most. We expect frequency to have a strong effect on the S-parameters. More specifically, we expect a large jump between low band and high band since the frequency jump is so large that the antenna most likely is using different excitation modes to radiate. In Figure 6, we see that this is exactly the case and that the low band behaves much worse than the high band. This is expected since the phone is electrically smaller at the lower frequencies making it harder to achieve good antenna performance for the low bands. As can be seen, approximately 75 % of the low band results fall above -6 dB which is often the acceptance criteria used for mobile phone antennas.

It can also be seen that the spread is a lot larger in the low band than the high indicating that the users affect the phone more in the low band. Looking at S_{21} in Figure 7, we see that S_{21} is generally very low. The median is below -30 dB for all frequencies. The frequency dependence is not strong.

If the data is divided into different power levels, it can be seen that S_{11} shows a strong correlation with output power level. Figure 8 shows that S_{11} is much worse and has a larger spread at lower power levels. The same can be seen in Figure 9 for S_{21}. This is not an expected outcome as the hypothesis

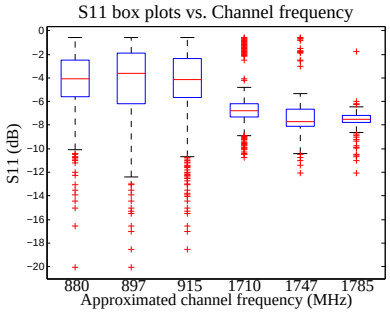

Fig. 6. Box plots for S_{11} versus estimated frequencies.

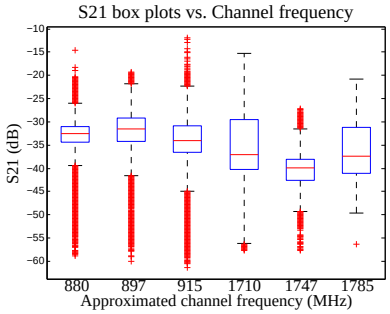

Fig. 7. Box plots for S_{21} versus estimated frequencies.

of the authors is that the antenna as a passive system should be power independent. One explanation can be that the phone is generally using lower powers in low band so that the effect seen is actually a second order effect caused by frequency dependency.

Based on the questionnaire data, different cross-sections of the data can be made. Here, it is chosen to look at the dependency of S_{11} and S_{21} on the gender of the test subject. The gender is parameter that is highly correlated with hand size and therefore it is expected that women with their smaller hands have less effect on the phone performance. Also, the grip style may generally be different between men and

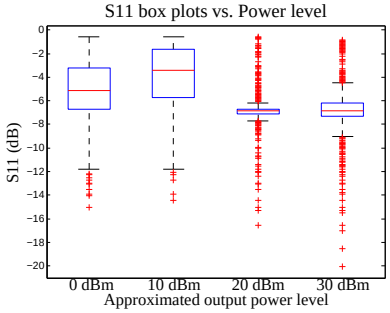

Fig. 8. Box plots for S_{11} versus estimated transmit power.

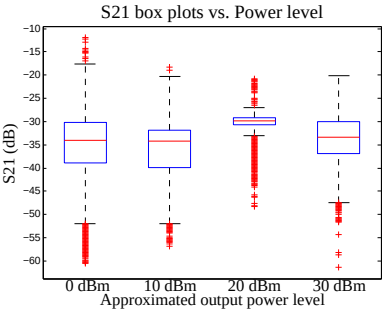

Fig. 9. Box plots for S_{21} versus estimated transmit power.

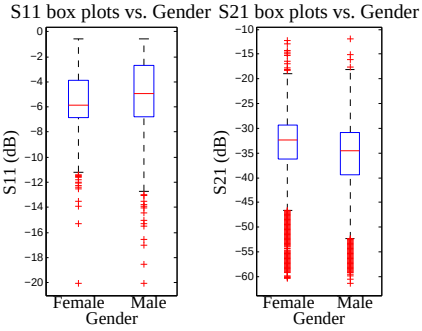

Fig. 10. Box plots for S_{11} and S_{21} as function of gender.

women. The data of Figure 10 support this hypothesis. For S_{11}, the reflection is less as well as the spread of the reflection coefficients. For S_{21}, the results from the women show slightly larger coupling and still with less spread. This indicates that the men with their bigger hands decouple the antennas more and that the decoupling effect is more dependent on their grip.

Not only the statistics of the user effect are of interest to the research community. Researchers and designers working on next generation antenna tuning should know the effect of the user on the antenna system to be able to specify the requirements for the tuning circuit. One part is to know the range of impedances seen by the transmitter as the antenna gets mismatched. This was covered in the results presented until now. Another important issue is the rate of change. If the user changes the grip on the phone then the S-parameters change and the system antenna tuning system has to keep up with these changes.

For this analysis the worst case events have been found and inspected. Figure 11 shows one of these events and the root cause found in the camera footage. It is observed that the test subject moves from a loose two-handed data grip to a one-handed grip. Before the grip change, nothing was touching the the sensitive points on the phone and the performance was therefore acceptable. After the grip change, the thumb is firmly pressed against the lower corners of the phone. This is the part of the antenna structure where the E-fields are strongest and therefore the place where the user affects the phone the most.

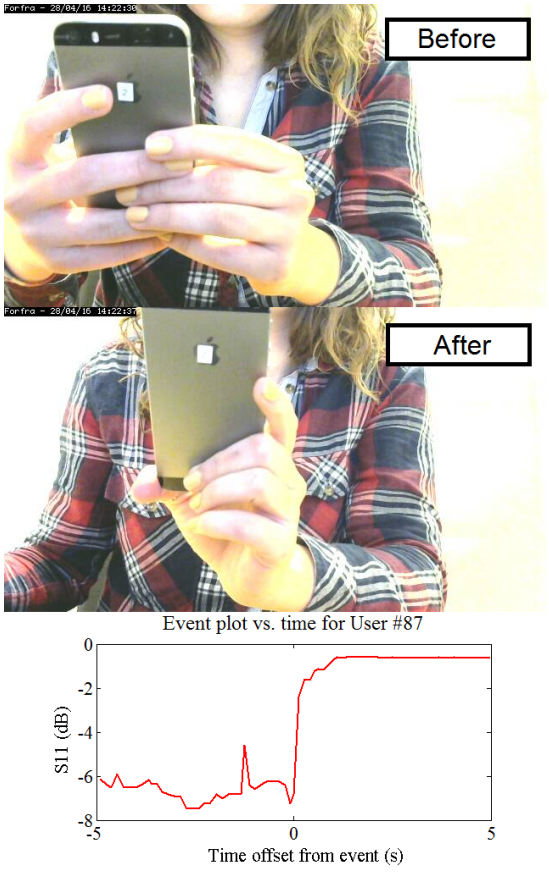

Fig. 11. Example of test subject moving the finger on to the high E-field region of the antenna and the associated change in S_{11}.

With the new grip the reflection coefficient is higher than -1 dB meaning that the antenna is almost completely reflecting the incoming power. Furthermore, the change happens very abruptly. The reflection coefficient changes from -6 to -2 in approximately 0.2 s. This gives an indication of the required bandwidth of a closed loop regulation if it were to regulate the iPhone 5s antenna.

Another event plot in Figure 12 shows a test subject changing positions in two steps. First step is comparable to the step seen in 11, just in the opposite direction. The reflection coefficient starts out for A) steadily at -1.6 dB due to the index finger being firmly pressed against the high-E-field region of the antenna. When the test subject loosens the grip, the reflection coefficient immediately falls to around -6 dB in B). The change from -2 to -6 dB is again taking around 0.2 s. Between B) and C), the test subject has once again moved the phone to his ear but is this time gripping only on the main part of the phone and not touching the antenna antenna itself. The step from -6 to -10 dB is happening very abruptly with a spike of -15 dB observed for on data point only. This indicates

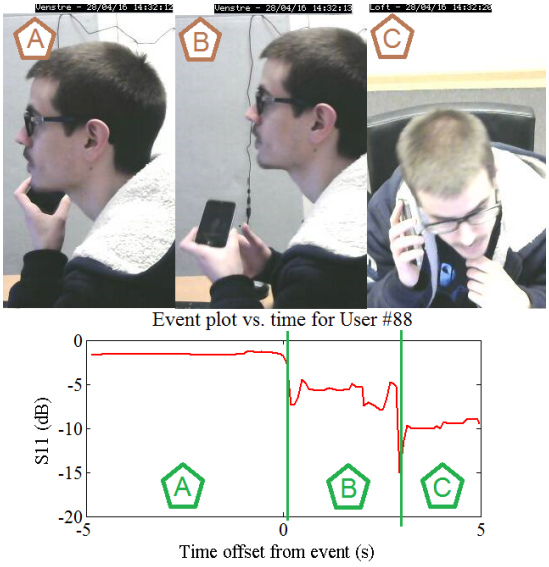

Fig. 12. Example of test subject moving the finger away from the high E-field region of the antenna and the associated change in S_{11}. The move happens in two steps where A) is before the steps, B) is between the steps and C) is after the steps.

that it has changed in 0.1 s or less.

The main data from the user study have now been presented. The following section will discuss what can be concluded based on the presented data.

IV. DISCUSSION

Through the course of the measurement campaign much new and previously unmeasurable data has been collected. The quality of the measurements is therefore not guaranteed. Therefore, the first step of the data processing was to filter away any questionable data. This can be done because for each measurement point an error indicator is calculated. This error indicator is not linear but has a complex dependency on the phase and amplitude of the S-parameter. Therefore, a cautious approach was taken and only data with a very low error value was used for the data analysis. This is not necessarily the correct way to filter the data as it may skew the results. If more data points are removed from certain regions due to the non-linearity of the error indicator then a fixed limit would lead to underrepresentation of this region in the statistics. Future implementations of TINAs should focus on much higher accuracy leading to more reliable data.

When analyzing the data it becomes clear that the coupling is always very low. This could indicate that the measurement of coupling is either erroneous or the iPhone 5s has very good isolation between its antennas. The measurement is however done on two separate phones that both yield the same results so it is repeatable.

For the reflection coefficient, results are more in line with expectations although they are generally not very good in low

band. It is possible to prove a dependence on the frequency of operation as well as the power level. For the gender, a weak but noticeable dependency is found. This is explained through the difference in hand size between men and women. A future study could directly measure the hand size and find the direct dependency between hand size and dynamic user effect.

The last part of the presented data is concerning the rate of change of S_{11}. Here the approach has been to take specific events and investigate their root cause based on the camera footage of the experiment. It was found that for the events with the highest rate of change, the user was changing the grip either placing or removing a part of the hand from the lower corners of the phone. These corners are known to be extremely sensitive in the iPhone 5s so this is what can be expected. In both of the highlighted events in this paper the reflection coefficient changes between -2 and -6 dB in 0.2 s which means that a closed loop tuning circuit must be even faster if these events should be prevented.

Both the range of S-parameters and the rate of change is very phone-dependent. The purpose of this measurement campaign was to obtain very early results in a field that has not been possible until now. It is thus not an in-depth study of the iPhone 5s in particular but rather a general study where the iPhone 5s was chosen as a test vessel because of prior experience with the phone and the massive popularity of the phone. If one chooses to use the data as a first estimate for specifying a closed loop antenna tuning system it is crucial to bear in mind that the dynamic user effect could be much different on another antenna system. Since the iPhone 5s has antennas integrated in the exterior of the phone it is likely to be more susceptible to direct contact with the antennas than phones with internal antennas. If a closed loop antenna tuning system can handle the iPhone 5s then it is most likely fast and versatile enough to handle most antenna systems.

One large limitation of the TINA that was used is that it can only measure in 2G mode. This means that the measurements are limited to the European 2G bands at 900 and 1800 MHz. If a system is designed that does not have this limitation, then the system will be much more versatile.

V. CONCLUSION

The application of the tiny integrated network analyzer, TINA, has enabled the researchers behind this study to capture very realistic data for the dynamics of the user effect of a mobile phone. These data would not have been accessible without the TINA. The amount of users makes this study very extensive and gives the researcher the ability to derive many statistical results from the study. There are still room for improvement in the measurement setup. A more accurate algorithm to identify faulty data would make the data processing much easier and mean that less of the good data is omitted from the analysis. For now, the researcher have chosen a cautious approach filtering out all data that is at all questionable.

Based on the remaining data it is seen that a) the coupling between the top and bottom antennas is always very low, b) the reflection coefficient is much higher, often worse than -6 dB, c) the low band is much worse than the high band, d) Lower power levels show worse performance than high power levels, e) There is a noticeable difference between male and female test subjects that can be explained by the difference in hand size. A future study could prove this by measuring the user effect directly as a function of hand size.

Finally the study gave an insight into the rate of change of S_{11}. For the iPhone 5s this study has found a high sensitivity to user interaction at the points where the antenna part of the bezel are closest to the metallic back plane of the phone. For all worst case events, the camera footage indicated that these points were touched either up to or just after the event. It is thus safe to say that these are the worst case points of the phone and that if a closed loop antenna tuning system can handle these changes then it is able to handle most events seen in modern smartphones. The requirement would be to be faster than 0.2 s at regulating a change from -6 dB to -2 dB.

REFERENCES

[1] A. Tatomirescu and G. Pedersen, "Body-loss for popular thin smart phones," in *Antennas and Propagation (EuCAP), 2013 7th European Conference on*, April 2013, pp. 3754–3757.

[2] A. Morris, Q. Gu, M. Ozkar, and S. Natarajan, "High performance tuners for handsets," in *Microwave Symposium Digest (MTT), 2011 IEEE MTT-S International*, June 2011, pp. 1–4.

[3] R. Whatley, T. Ranta, and D. Kelly, "RF front-end tunability for LTE handset applications," in *Compound Semiconductor Integrated Circuit Symposium (CSICS), 2010 IEEE*, Oct 2010, pp. 1–4.

[4] A. van Bezooijen, M. de Jongh, F. van Straten, R. Mahmoudi, and A. van Roermund, "Adaptive impedance-matching techniques for controlling l networks," *Circuits and Systems I: Regular Papers, IEEE Transactions on*, vol. 57, no. 2, pp. 495–505, Feb 2010.

[5] M. de Jongh, A. van Bezooijen, K. Boyle, and T. Bakker, "Mobile phone performance improvements using an adaptively controlled antenna tuner," in *Microwave Symposium Digest (MTT), 2011 IEEE MTT-S International*, June 2011, pp. 1–4.

[6] 3GPP, "LTE; user equipment (UE) / mobile station (MS) over the air (OTA) antenna performance; conformance testing," 3GPP, Tech. Rep. 3GPP TS 34.114 version 12.1.0, September 2014.

[7] CTIA Certification Program, "Test plan for wireless device Over-the-Air performance," CTIA, Tech. Rep. Rev 3.4, December 2014.

[8] R. Lao, W. Liang, Y.-S. Chen, and J. Tarng, "The use of electro-optical link to reduce the influence of RF cables in antenna measurement," in *Microwave, Antenna, Propagation and EMC Technologies for Wireless Communications, 2005. MAPE 2005. IEEE International Symposium on*, vol. 1, Aug 2005, pp. 427–430 Vol. 1.

[9] B. Yanakiev, J. Nielsen, M. Christensen, and G. Pedersen, "Long-range channel measurements on small terminal antennas using optics," *Instrumentation and Measurement, IEEE Transactions on*, vol. 61, no. 10, pp. 2749–2758, Oct 2012.

[10] S. Saario, D. Thiel, J. Lu, and S. O'Keefe, "An assessment of cable radiation effects on mobile communications antenna measurements," in *Antennas and Propagation Society International Symposium, 1997. IEEE., 1997 Digest*, vol. 1, July 1997, pp. 550–553 vol.1.

[11] E. F. Buskgaard, B. K. Kryer, A. Tatomirescu, O. Franek, and G. F. Pedersen, "Tiny integrated network analyzer for noninvasive measurements of electrically small antennas," *IEEE Transactions on Microwave Theory and Techniques*, vol. 64, no. 1, pp. 279–288, Jan 2016.

ISSN (online): 2246-1248
ISBN (online): 978-87-7112-848-2

AALBORG UNIVERSITY PRESS